



Possible use as biofuels of monoaromatic oxygenates produced by lignin catalytic conversion: A review

Frederique Battin-Leclerc, N. Delort, I. Meziane, Olivier Herbinet, Y. Sang, Y. Li

► To cite this version:

Frederique Battin-Leclerc, N. Delort, I. Meziane, Olivier Herbinet, Y. Sang, et al.. Possible use as biofuels of monoaromatic oxygenates produced by lignin catalytic conversion: A review. Catalysis Today, 2023, 408, pp.150-167. 10.1016/j.cattod.2022.06.006 . hal-03853384

HAL Id: hal-03853384

<https://hal.science/hal-03853384>

Submitted on 15 Nov 2022

HAL is a multi-disciplinary open access archive for the deposit and dissemination of scientific research documents, whether they are published or not. The documents may come from teaching and research institutions in France or abroad, or from public or private research centers.

L'archive ouverte pluridisciplinaire **HAL**, est destinée au dépôt et à la diffusion de documents scientifiques de niveau recherche, publiés ou non, émanant des établissements d'enseignement et de recherche français ou étrangers, des laboratoires publics ou privés.

POSSIBLE USE AS BIOFUELS OF MONOAROMATIC OXYGENATES PRODUCED BY LIGNIN CATALYTIC CONVERSION: A REVIEW

F. Battin-Leclerc^{1*}, N. Delort¹, I. Meziane¹, O. Herbinet¹, Y. Sang², Y. Li²

¹*Univ. Lorraine, CNRS, UMR 7274 - LRGP - Laboratoire Réactions et Génie des Procédés, F-54000, Nancy, France*

²*Department of Chemical & Metallurgical Engineering, School of Chemical Engineering, Aalto University, Kemistintie 1, Espoo, 02150 Finland*

Published in *Catalysis Today* 408 (2023) 150–167
<https://doi.org/10.1016/j.cattod.2022.06.006>

Abstract

Small aromatic molecules with oxygen-containing functional groups (monoaromatic oxygenates) are common products of the catalytic depolymerization of lignin, which can be considered as a promising class of fuel additives. This mini-review article starts with an introduction of second generation (2G) of biofuel production from lignocellulose and the further conversion of lignin into fuel performance boosting blends. The discussion is divided into four parts. The first part gives a brief overview of the production of aromatic oxygenates from the catalytic conversion of lignin of different origin. The three following parts are focused on the aromatic oxygenates, for which combustion data can be found. The second part describes their chemical structure and physical properties. The third part is dominated by their global combustion performance, i.e., the commercial fuel parameters as lower heating value, octane and cetane numbers. A few studies on ignition delay times and laminar flame velocities are also described. The fourth part shortly reviews the kinetic studies presenting product quantifications, the proposed detailed kinetic models and the influence of the structure of the aromatic reactant on soot formation. To finish, a perspective on future research directions is given.

Keywords: Lignin; catalytic depolymerization; aromatic oxygenates in biofuel; combustion; chemical kinetics.

* Corresponding author: frederique.battin-leclerc@univ-lorraine.fr

Introduction

The urgent need to decrease CO₂ emission has led researchers to more and more consider the ways of using biomass to produce chemicals, transportation fuels and energy. With the purpose of producing fuels for various combustion applications, lignocellulosic biomass transformation technologies have been actively developed via a number of routes, such as gasification to produce synthesis gas (at reaction temperatures from 1050 to 1300 K) for the synthesis of liquid fuel and chemicals [1], fast pyrolysis yielding bio-oil as a precursor to liquid fuel (from 700 to 1000 K) [2], and enzymatic hydrolysis fermentation to utilize the sugars from cellulose to produce bioethanol and biogas, which is as so called second generation (2G) biofuel [3].

Lignocellulosic biomass is mainly composed of three heterogeneous polymers, cellulose, hemicellulose and lignin, the structures of them are displayed in Figure 1. While cellulose and hemicellulose are constituted of five- and six-membered saturated cyclic ethers, lignin is rich with aromatic rings. In the three structures, the cycles are repeatedly linked to oxygenated functional groups, mainly hydroxy (OH) and methoxy (CH₃O) ones. In 2G biofuel processes, cellulose and hemicellulose are transformed firstly into hexose and pentose, and the hexose and pentose are subsequently transformed to biofuels, i.e., methane or ethanol, leaving lignin as a promising feedstock for aromatics and oxygenated aromatics, which are highly demanded by chemical industry and as fuel boosters.

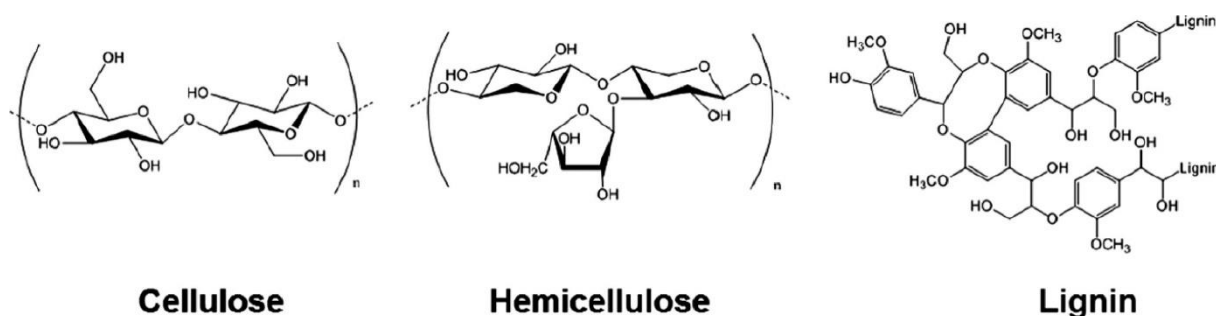


Figure 1: Structure of the major components of lignocellulosic biomass – reprinted from [4] with the permission of Elsevier.

Depending on its original biomass, lignin can contain different proportions of the following three types of oxygenated phenyl-propane units, p-hydroxyphenyl (H-unit, with the benzene ring link to an OH group), guaiacyl (G-unit, with the benzene ring link to a hydroxy and a methoxy groups), syringyl (S-unit, with the benzene ring link to a hydroxy and two methoxy groups) linked by C-C or ether bonds.

Several essential industrial processes rely on the transformation of the cellulosic part of biomass with lignin being a byproduct mostly treated as a waste or burnt. Paper industry produces 50

million tons of lignin annually, with only 2% of it being valorized [5]. Enzymatic hydrolysis lignin (EHL) is the solid residue formed during the production of (2G) biofuels, especially bioethanol, from lignocellulosic biomass by fermentation [6].

In the last fifteen years, an increasing range of catalytic processes have been proposed to transform biomass that is not used for food production in a wide range of molecules of interest [5,7,8]. Figure 2 presents the general strategy proposed for upgrading lignocellulosic biomass by catalytic processes to produce chemicals and biofuels, which consists, as well explained by Dumesic and co-authors [7], in removing the O-atoms in order to decrease the boiling point and increase the heating value.

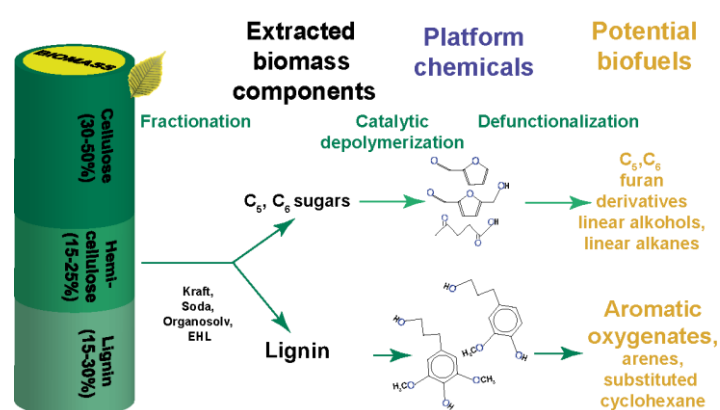


Figure 2: Strategy of lignocellulosic biomass upgrading to fuels by catalytic processes [5,8].

According to this strategy, biomass is first fractionated to separate lignin from the cellulosic part. Several fractionation processes were proposed [5], e.g. Kraft, soda, organosolv, EHL..., and were especially focused on obtaining high quality cellulose. Depending on the aggressiveness of the used reactants, from strong bases, such as sodium hydroxide and sulfite in the Kraft process, to enzymes for EHL, the native structure of lignin is more or less degraded during this fractionation process. Following fractionation, catalytic processes, e.g. hydrolysis or solvolysis, dehydration, double bond hydrogenation, are used to depolymerize sugars [5] or lignin [5] and to produce platform chemicals (see figure 2), which can be catalytically transformed to the target molecules. The C₅-C₆ sugars obtained from the cellulosic part of biomass can yield furan derivatives, molecules with promising perspectives as transportation fuel, or in more classical linear alcohols and alkanes [9].

Concerning lignin, as described in the part 1 of the present paper, according to the origin and the used catalytic processes, the derived potential molecules in fuel range are to be found amongst aromatic oxygenates or hydrocarbons such as aromatic hydrocarbons (arenes) and substituted cyclohexanes, which are usual components of fossil fuels [10]. In order to help considering the question on how far the catalytic processes should go in removing O-atoms, the

purpose of this paper is to examine several points of interest for using aromatic oxygenates in combustion processes, such as internal combustion engines, gas turbines or burners. Their thermodynamic properties (change of state) are considered in the part 2, their global combustion parameters, including both reactivity indicators and sooting tendency, are discussed in part 3, and finally the experimental and kinetic studies related to their pollutant emissions during combustion are reviewed in the part 4.

1. Catalytic processes producing small molecules from lignin

The pyrolysis and gasification of lignin without solvent were investigated in early works, yielding gases (CO, CO₂, H₂ and gaseous hydrocarbons), liquid oil (phenolic compounds, methanol, acetone, acetaldehyde and water as well as oligomers and large fragments) and char [11,12]. Although lignin pyrolysis and gasification have achieved commercial-scale demonstration, catalytic lignin depolymerization in a solvent, i.e., catalytic lignin solvolysis (CLS), is more promising, as it directly produces high-value small-molecular products without or with little formation of char. The works reported on CLS are sorted into three categories: reductive and oxidative CLS, and acid/base-catalyzed reactions [5,13]. In oxidative CLS, acids and esters with high oxygen content are usually produced, which are suitable for use as chemicals, instead of fuel. In acid/base-catalyzed reactions, repolymerization reactions are also promoted, resulting in the formation of chars, especially at a high reaction temperature. In order to suppress the formation of char and improve the lignin conversion, acid/base functions are incorporated with hydrogenation sites. In reductive CLS or acid/base promoted reductive CLS, lignin depolymerization and product hydrodeoxygenation occur simultaneously, yielding molecules as suitable precursors of fuels. Therefore, reductive CLS is discussed in some detail within this context. The typical small molecules, close to fuel range, derived from reductive CLS are listed in Figure 3.

An important factor that affects the product distribution is the fractionation technology of lignin. Large amounts of arenes are produced from CLS of pulping process derived lignin, such as Kraft, alkaline and soda lignin, as the structures of these lignin have been significantly modified during the pulping process [22] [24]. Organosolv lignin and enzymatic hydrolysis lignin are less modified, and their structures are similar to native lignin, and the primary monomers derived from these types of lignin are mostly para-substituted phenols [18] [27,28].

The product distribution also depends on the catalyst and solvent used as well as CLS reaction conditions (with or without H₂). Without H₂, alcohol solvents, especially methanol, ethanol and isopropanol, provide active hydrogen for CLS, with themselves converting to aliphatic oxygenates, such as higher alcohols, esters and ethers [14–17]. The intermediates of alcohol self-conversion also react with those formed from lignin depolymerization reaction, forming

alkyl and alkoxy groups substituted aromatic monomers [14]. Actually for many molecules found in the product, the pieces from the alcohol are quite obvious. Therefore, complex aliphatic and aromatic products are usually obtained in reductive CLS with alcohols as hydrogen-donors. Some milestone works achieved complete lignin liquefaction and high monomer yields [6,18–23]. Barta *et al.* [18] converted organosolv lignin into cyclohexane derivatives with CuMgAlO_x mixed oxide as a catalyst in methanol at 573 K under Ar atmosphere. Huang *et al.* [24] employed similar CuMgAlO_x as a catalyst for depolymerization of Kraft lignin in ethanol at 653 K for 6 h in N_2 , yielding 86 wt% monomer products which mainly include cyclohexane derivatives, arenes and alkylated phenols. Ma *et al.* [22] reported that $\text{MoC}_{1-x}/\text{C}$ catalyst achieved the complete conversion of Kraft lignin in ethanol and obtained 1.64 g/g lignin of small molecules, including both aromatic products (arenes, benzyl alcohols and phenols) and aliphatic products (alcohols, esters and ethers), at 553 K for 6 h in N_2 . Similar products were obtained from $\text{Mo}/\text{Al}_2\text{O}_3$ and $\text{Mo}_2\text{N}/\text{Al}_2\text{O}_3$ catalyzed Kraft lignin depolymerization [14]. Mai *et al.* [25] employed $\text{WO}_3/\delta\text{-Al}_2\text{O}_3$ as a catalyst for the depolymerization of EHL in ethanol at 593 K for 8 h under N_2 atmosphere, and obtained 31.5 wt% of aromatic monomers. $\text{WO}_3/\delta\text{-Al}_2\text{O}_3$ shows high activity for alkylation and etherification reaction, yielding alkylated and etherified phenols as main products. When CLS is carried out in alcohol under H_2 pressure, solvent self-conversion and second conversion of primary monomers are suppressed, and para-substituted phenols, which are directly derived from lignin units, are the main products. Ni and noble metal (Pt, Pd, Ru) as catalysts with high hydrogenation activities usually produce para-alkyl and para-propanol phenols as the main products. For example, Sang *et al.* [27,28] prepared an unsupported nickel-based catalyst via nickel formate decomposition, and employed it for EHL depolymerization in ethanol. After reaction at 553 K under 2 MPa H_2 for 6 h, 28.5 wt% of monomers, mainly including para-alkyl phenols, para-propanol phenols and esters derived from ferulic and p-coumaric acids, were obtained. Xiao *et al.* [26] reported that MoO_3 supported on carbon nanotubes (MoO_3/CNT) also mainly produces para substituted phenols in depolymerization of enzymatic mild acidolysis lignin in methanol under 3 MPa H_2 . Different from Ni and noble metal catalysts, MoO_3/CNT show lower activity for hydrogenation of the carbon-carbon double bonds in para-side chains, and hence para-alkenyl phenols are the main products.

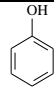
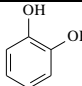
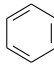
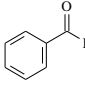
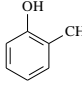
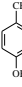
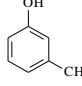
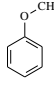
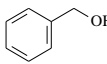
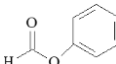
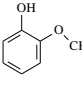
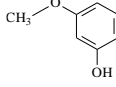
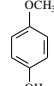
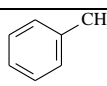
Different from oxygenated solvents, cycloalkanes and alkanes are the main products in the case with alkanes as solvents [29]. For example, Kong *et al.* [30] reported that phenolic monomers were produced in oxygenated solvents, including ethylene glycol, dioxane, ethanol and tetrahydrofuran, but cycloalkanes and alkanes were the main products in dodecane, in $\text{Ni}/\text{Al}_2\text{O}_3\text{-SiO}_2$ catalyzed EHL depolymerization at 523 K under 4 MPa H_2 . Li and his co-workers [31,32] also reported that EHL was depolymerized into alkylated cyclohexane with cyclohexane as a solvent and $\text{NiMo}/\text{Al}_2\text{O}_3$ as a catalyst at 593 K under 2.7 MPa H_2 , but phenolic monomers were produced in ethanol with the same catalyst under the same reaction conditions. Nevertheless,

Aliphatic Products				Aromatic Products			
Alcohols				Alkyl/alkenyl substituted benzenes (arenes)		Alkylated Phenols	
Esters				Benzyl Alcohols		Etherified Phenols	
Ethers				para-Alkyl and Alkenyl Phenols		Phenols without Side Chains	
Cyclohexane Derivatives				para-Propanol Phenols		Esters	

2. Chemical structure and thermodynamic properties of the aromatic oxygenates discussed in this paper

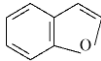
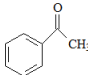
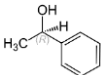
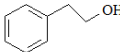
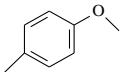
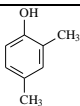
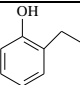
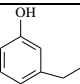
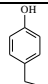
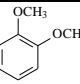
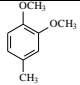
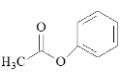
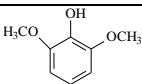
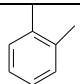
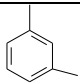
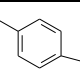
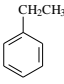
6

Table 1: Name, formula, structure, molecular weight (MW) and density of the C₆-C₇ aromatic oxygenates discussed in this paper.

Specie n ^o	Common name	Molecular formula	Chemical Structure	MW g/mol	Density (298 K) kg/m ³	
					Value	Ref
1	phenol	C ₆ H ₆ O		94.1	1065	[34,35]
2	catechol	C ₆ H ₆ O ₂		100.1	1344 ¹	[36]
3	benzene	C ₆ H ₆		78.1	855	[35]
4	benzaldehyde	C ₇ H ₆ O		106.1	1014	[35]
5	o-cresol	C ₇ H ₈ O		108.1	1028	[35]
6	p-cresol			108.1	1140	[34,35]
7	m-cresol			108.1	1030	[35]
8	anisole	C ₇ H ₈ O		108.1	980	[34,35,37]
9	benzyl alcohol	C ₇ H ₈ O		108.1	1041	[35]
10	phenyl formate	C ₇ H ₆ O ₂		122.1	1155	[35]
11	o-guaiacol	C ₇ H ₈ O ₂		124.1	1129	[34,38]
12	m-guaiacol			124.1	1145	[39]
13	p-guaiacol			124.1	1550 ¹	[40]
14	toluene	C ₇ H ₈		92.1	862	[35,41]

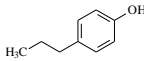
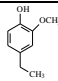
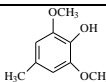
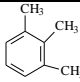
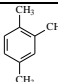
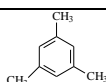
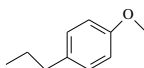
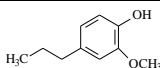
¹ density at 293 K.

Table 2: Name, formula, structure, molecular weight and density of the C₈ aromatics oxygenates discussed in this paper.

Specie n°	Common name	Molecular formula	Chemical Structure	MW g/mol	Density (298 K) kg/m ³	
					Value	Ref
15	benzofuran	C ₈ H ₆ O		188.1	1095 ¹	[40]
16	acetophenone	C ₈ H ₈ O		120.1	1028	[33]
17	1-phenyl ethanol	C ₈ H ₁₀ O		122.2	1012	[40]
18	2-phenyl ethanol	C ₈ H ₁₀ O		122.2	1021 ¹	[39,40,42]
19	4-methylanisole	C ₈ H ₁₀ O		122.2	969	[34]
20	2,4-xlenol	C ₈ H ₁₀ O		122.2	1011	[34]
21	o-ethylphenol	C ₈ H ₁₀ O		122.2	963	[35]
22	m-ethylphenol	C ₈ H ₁₀ O		122.2	1001	[40]
23	p-ethylphenol	C ₈ H ₁₀ O		122.2	933	[35]
24	1,2-dimethoxybenzene	C ₈ H ₁₀ O ₂		138.2	1084	[34]
25	4-methylguaiacol	C ₈ H ₁₀ O ₂		138.2	1092	[34]
26	phenyl acetate	C ₈ H ₈ O ₂		136.2	1093	[35]
27	2,6-dimethoxyphenol	C ₈ H ₁₀ O ₃		154.2	1134	[34]
28	<i>o</i> -xylene	C ₈ H ₁₀		106.2	870	[35,43]
29	<i>m</i> -xylene	C ₈ H ₁₀		106.2	855	[35,43]
30	<i>p</i> -xylene	C ₈ H ₁₀		106.2	849	[35,43]
31	ethylbenzene	C ₈ H ₁₀		106.2	855	[35,43]

¹ density at 293 K.

Table 3: Name, formula, structure, molecular weight and density of the C₉-C₁₀ aromatics oxygenates discussed in this paper and of standard fuels.

Specie n°	Common name	Molecular formula	Chemical Structure	MW g/mol	Density (298 K)	
					kg/m ³ Value	Ref
32	4-propylphenol	C ₉ H ₁₂ O		136.2	983	[34]
33	4-ethylguaiacol	C ₉ H ₁₂ O ₂		152.2	1063	[34]
34	4-methyl-2,6-dimethoxyphenol	C ₉ H ₁₂ O ₃		168.2	1050	[34]
35	<i>1,2,3-trimethylbenzene</i>	<i>C₉H₁₂</i>		120.2	891	[35]
36	<i>1,2,4-trimethylbenzene</i>	<i>C₉H₁₂</i>		120.2	857	[35]
37	<i>1,3,5-trimethylbenzene</i>	<i>C₉H₁₂</i>		120.2	842	[35]
38	4-propylanisole	C ₁₀ H ₁₄ O		150.2	941	[34]
39	4-propylguaiacol	C ₁₀ H ₁₄ O ₂		166.2	1038	[34]
-	<i>gasoline</i>	<i>C₅-C₁₁</i>	-	60-140	720-775 ²	[44]
-	<i>diesel fuel</i>	<i>C₁₂-C₂₅</i>	-	150-350	820-845 ²	[45]

² Standardized value of density at 288 K.

Tables 1 to 3 also include a few arenes and standard fuels (in italic in these tables), for which thermodynamic and combustion properties are given for comparison. Other properties, such as viscosity or solubility, not given in Table 1 to 3, would need to be further considered for using a molecule in combustion processes. Note that aromatic oxygenates are frequently used in the flavor and fragrance industry and thus considered of low toxicity [33]. Table 1 to 3 well shows how the presence of oxygen atoms increases density at 298 K, which is around 1000 kg/m³ for aromatic oxygenates and only around 850 kg/m³ for arenes. Anisole and 4-methylanisole have a density (at 298 K) slightly below 1000 kg/m³, while those of p-cresol, phenyl formate, guaiacol isomers, and 2,6-diethoxyphenol are above 1100 kg/m³. According to [10], the recommended density for gasolines (at 298 K) is in the range 712-767 kg/m³, however McCormick et al. [34] indicated that blending of the oxygenates had little impact on gasoline density.

Table 4 displays the phase change data (boiling point, melting point, vapor pressure and heat of vaporization) of the aromatic compounds displayed in Tables 1 to 3. As indicated by Table 4, the temperatures for phase transition of aromatic oxygenates are not favorable for use in engines and gas-phase kinetic studies. Most of those compounds, even C₆-C₇ ones such as phenol, catechol, and two isomers of cresols, are solid at room temperature. Despite its melting point of 301 K, when used in a laboratory, o-guaiacol is liquid, or a solid/liquid mixture depending on the room temperature.

Only three compounds in Table 4 have a vapor pressure under standard conditions above 1×10^{-3} bar: anisole, 1,2-dimethoxybenzene and 4-propylanisole. This explains the large number of kinetic studies related to anisole as detailed further in the text. A maximum boiling temperature of 483 K is imposed (EN 228 [44]) for an additive to be considered in gasoline, therefore only phenol, benzaldehyde, cresol isomers, anisole, benzyl alcohol, o-guaiacol, benzofuran, acetophenone, 1-phenylethanol, 4-methylanisole, 1,2-dimethoxybenzene and o-ethylphenol are in the validity range. In contrast to the aromatic oxygenates, all the arenes listed in Tables 1 to 3 are liquid at room temperature and can be easily vaporized.

Table 4: Phase change data (boiling point (T_{boil} at 1 bar in K), melting point (T_{melt} at 1 bar in K), vapor pressure under standard conditions (P_{vap} at 1 atm in bar) and heat of vaporization (H_{vap} at 298 K in kJ/mol) of the aromatic compounds displayed in Tables 1 to 3. Boiling point in bold are above 483 K, melting points in bold are above room temperature (298 K), vapor pressure in bold are above $1 \times 10^{-3} \text{ bar}$.

Name	T_{boil}	T_{melt}	P_{vap}	H_{vap}
phenol	455 [34,35,46]	314 [34,46]	6.38×10^{-4} [35]	583.7 [35]
catechol	519 [35,46]	377 [46]	3.57×10^{-6} [35]	696.2 [35]
benzaldehyde	452 [35,46]	231 [46]	1.66×10^{-3} [35,46]	462.1 [35]
o-cresol	464 [35,46]	304 [46]	4.88×10^{-4} [35]	508.9 [35]
p-cresol	475 [34,35,46]	307 [34,46]	1.89×10^{-4} [35]	548.8 [35]
m-cresol	475 [35,46]	284 [46]	2.74×10^{-4} [35]	526.4 [35]
anisole	427 [34,35,38,46–48]	250 [34,46]	4.28×10^{-3} [35]	425.9 ± 6.2 [35,46,47,49,50]
benzyl alcohol	478 [35,46]	257 [46]	4.82×10^{-5} [35]	610.6 [35]
phenyl formate	523 [35]	--	7.72×10^{-6} [35]	579.2 [35]
o-guaiacol	478 [34,35,38,46,48]	301 [34,46]	1.29×10^{-4} [35]	494.4 [35]
m-guaiacol	517 [46]	256 [39]	1.50×10^{-4} [42]	393.7^2 [51]
p-guaiacol	516 [35,46]	326 [46]	1.83×10^{-5} [35]	540.6 [35]
benzofuran	455 [46]	255 [40]	1.24×10^{-2} [52]	350.2^2 [51]
acetophenone	475 [35,46]	293 [46]	7.64×10^{-4} [35]	438.6 [33]
1-phenylethanol	476 [46]	291 [46]	7.50×10^{-4} [42]	382.9^2 [51]
2-phenylethanol	493 [46–48]	254 [46]	1.16×10^{-6} [53]	562.9 ± 2.7 [47,54,55]
4-Methylanisole	448 [46]	242 [46]	-- --	317.1^2 [51]
1,2dimethoxybenzene	480 [46]	294 [46]	3.53×10^{-3} [42,56]	492.9 [46]
2,4-xylene	484 [46]	298 [46]	1.31×10^{-4} [35,57]	510.3 [35,57]
o-ethylphenol	478 [35,46]	280 [46]	3.09×10^{-4} [35]	581.3 [35]
m-ethylphenol	490 [35,46]	269 [46]	3.75×10^{-4} [58]	398.6^2 [51]
p-ethylphenol	491 [35,46]	319 [46]	9.34×10^{-5} [35]	504.2 [35]
phenyl acetate	469 [46]	243 [40,42]	3.06×10^{-4} [35]	395.1 ± 8.2 [35,46]
4-propylanisole	489 [46]	268 [34]	2.00×10^{-3} [59]	287.6^2 [51]
4-methylguaiacol	494 [46]	278 [34]		513.2 [60]
4-propylphenol	505 [46]	295 [46]	2.80×10^{-5} [42]	373.9^2 [51]
4-ethylguaiacol	508 [39]	288 [34]	-- --	354.8^2 [51]
4-propylguaiacol	523 [39]	289 [46]	-- --	338.2^2 [51]
2,6-dimethoxyphenol	536 [46]	328 [34]	-- --	380.3^2 [51]
4-methyl-2,6-dimethoxyphenol	541 [34]	273 [34]	-- --	365.7^2 [51]
benzene	353 [35,46]	279 [46]	1.24×10^{-1} [35,46]	402.3 [35,46]

<i>toluene</i>	383	[35,38,4 6,48]	178	[46]	3.73×10^{-2}	[35,46]	408.0 ± 4.1	[35,46,54,55]
<i>o-xylene</i>	417	[35,46]	248	[46]	8.58×10^{-3}	[35,46]	403.6	[35]
<i>m-xylene</i>	412	[35,46]	225	[46]	1.07×10^{-2}	[35,46]	398.1	[35]
<i>p-xylene</i>	411	[35,46]	286	[46]	1.13×10^{-2}	[35,46]	396.9 ± 2.1	[35,46,47,54,55]
<i>ethylbenzene</i>	409	[35,46]	179	[46]	1.25×10^{-2}	[35]	413.2 ± 34.5	[46,54,55]
<i>1,2,3-trimethylbenzene</i>	449	[35,46]	248	[46]	1.84×10^{-3}	[35]	404.0	[35]
<i>1,2,4-trimethylbenzene</i>	442	[35,46]	228	[46]	2.49×10^{-3}	[35]	395.4	[35]
<i>1,3,5-trimethylbenzene</i>	438	[35,46]	226	[46]	2.85×10^{-3}	[35]	394.1	[35]

¹ Vapor pressure at 293 K, ² calculated with Joback's method [51], ³ values of petroleum fuel compounds,

⁴Standards on vapor pressure range depend on locations in Europe, ⁵Standardized final boiling point.

3. Global combustion parameters of aromatic oxygenates

This part aims at giving an idea on how aromatic oxygenates perform when used in internal combustion engines, first listing the data which can be found for the usual global indicators of combustion and ignition performances, the Lower Heating Value (LHV), Research Octane Number (RON) and Cetane Number (CN), and then reviewing the few studies presenting measurements of ignition delay times and laminar flame velocities.

3.1. Global indicators of combustion and ignition performances

In addition to the LHV, which gives an idea of the fuel energy density, two numbers are used to characterize the fuel auto-ignition performances, the octane number (often RON), which rates the fuel resistance to auto-ignition [9], and the Cetane Number (CN) [10], which in contrast rates the fuel ignitibility. These ignition parameters are established thanks to European (respectively American) standard test methods EN ISO 5164 [10] (resp. ASTM D2699) for RON and EN ISO 5165 [10] for CN (resp. ASTM D613); American and European test methods have the same specifications. A new ASTM method was recently developed: ASTM D 6890, in order to measure CN with a very little amount of sample; the obtained property is called "Derived Cetane Number". Standard fuel properties are given by EN 228 [44] (resp. ASTM D4814) for gasoline and EN 590 [45] (resp. ASTM D975) for Diesel. A large amount of studies was performed in order to predict and interpolate these parameters thanks to analytical formulae or numerical methods like artificial neural networks, e.g. [61–68] but no obvious correlation with structure or other properties of molecules was found to be accurate on a wide variety of families or on a large range of RON and CN.

Table 5 presents the data, which can be found in literature for LHV, RON and CN. Both mass and volume LHVs are given, since the first ones are of importance for aviation and the second ones for ground transportation. It is clear from this table, that concerning LHVs, a major

drawback of aromatic oxygenates is their lower values compared to their non-oxygenated counterpart species. Only 2-phenyl ethanol and 4-propylanisole have a LHV above 35 MJ/kg, while C₇-C₉ arenes have LHVs around 41 MJ/kg in the same range as gasoline indicating that removing oxygen atoms on typical lignin derived compounds would allow obtaining the same properties as traditional fuels. However, thanks to their high density, these oxygenated species have a volumetric LHV in the range of petroleum fuel values, what leads to the same fuel consumption.

Experimental octane and cetane numbers are rare in literature for neat aromatic oxygenates, however these compounds were tested as additives in gasolines up to 20%, see for instance [34,38,47,49,69–71]. According to the few existing data for neat compounds, aromatic oxygenates, as aromatic hydrocarbons, have a high octane number (RON >100 for all the molecules for which this value was found), and conversely a low cetane number (CN<30), making them potential octane booster in spark ignited engines to upgrade performances of gasolines.

In traditional gasolines, arenes are the compounds with the highest RONs and oxygenated aromatics have ignition properties in the same range of values. However, as it is described before, what limits the use of oxygenated compounds as drop-in gasoline blend components is their high boiling temperatures.

Table 5: Lower heating value (LHV), research octane number (RON) and cetane number (CN) of aromatic oxygenates of the compounds listed in Tables 1 to 3. Mass LHVs in bold are above 35 MJ/kg.

Names	LHV			RON		CN	
	Value MJ/kg	Value MJ/L	Ref	Value	Ref	Value	Ref
phenol	31.3	33.3	[34]	--	--	--	--
catechol	27.7 ¹	37.2	[51]	--	--	--	--
benzaldehyde	32.1 ²	32.5	[46]	--	--	--	--
o-cresol	32.7 ²	33.6	[46,72]	--	--	--	--
m-cresol	32.8 ²	33.8	[46,72]	--	--	--	--
p-cresol	29.6	33.7	[34]	153	[34]	--	--
anisole	33.7 ± 0.3	33.0	[34,37,38,47–50,73,74]	114 ± 10	[34,38,47,50,75]	6 ± 1	[34,38,50,62]
benzyl alcohol	34.6	36.0	[69]	--	--	29	[69]
o-guaiacol	27.5	31.0	[34,38,48,73]	--	--	19	[34,38,62]
m-guaiacol	27.5 ¹	31.5	[51]	--	--	--	--
p-guaiacol	27.3 ¹	42.3	[51]	--	--	--	--
benzofuran	32.6 ²	35.7	[46]	--	--	--	--
acetophenone	33.2	34.2	[33]	--	--	--	--
1-phenylethanol	29.0 ¹	29.3	[51]	--	--	--	--

2-phenylethanol	35.0 ± 1.4	35.6	[47,48,54,55,73]	116 ± 11	[34,38,47,55]	8	[34,62]
4-methylanisole	34.4	33.3	[34]	104	[38]	7	[38]
1,2-dimethoxybenzene	27.4	29.7	[34]	--	--	17	[34]
2,4-xylene	33.8	34.2	[34]	140	[34]	--	--
o-ethylphenol	34.1 ²	32.8	[46]	--	--	--	--
m-ethylphenol	34.1 ²	34.1	[46]	--	--	--	--
p-ethylphenol	33.9 ¹	31.6	[51]	--	--	--	--
4-propylanisole	36.4	34.3	[34]	--	--	8	[38]
4-methylguaiacol	28.9	31.6	[34]	--	--	20	[38]
4-propylphenol	34.8	34.2	[34]	--	--	9	[34]
4-ethylguaiacol	28.7	30.5	[34]	--	--	20	[38]
4-propylguaiacol	31.5	32.7	[34]	--	--	18	[34]
2,6-dimethoxyphenol	25.2	28.6	[34]	--	--	26	[34]
4-methyl-2,6-dimethoxyphenol	27.7	29.1	[34]	--	--	25	[34]
<i>benzene</i>	40.3²	34.5	[46]	102 ± 5	[76,77]	14	[78]
<i>toluene</i>	40.9 ± 0.4	35.3	[38,54,55,73,79]	116 ± 10	[34,50,73,76,77,80–82]	6 ± 3	[38,50,62,76,78]
<i>o-xylene</i>	40.9 ± 0.1	35.6	[79,83,84]	113 ± 8	[48,76,77]	8	[76,78]
<i>m-xylene</i>	41.4 ± 0.6	35.4	[79,83,84]	122 ± 21	[48,76,77]	7	[76,78]
<i>p-xylene</i>	41.5 ± 0.5	35.2	[47,48,54,55,79]	121 ± 18	[48,76,77,80]	6	[76,78]
<i>ethylbenzene</i>	41.6 ± 0.4	35.6	[54,55,79]	108 ± 8	[38,38,54,55,76,80]	6	[76,78]
<i>1,2,3-trimethylbenzene</i>	41.2²	36.7	[46]	110 ± 9	[50,76,77]	10	[76,78]
<i>1,2,4-trimethylbenzene</i>	41.2²	35.1	[46]	148	[77]	9	[50,76,78]
<i>1,3,5-trimethylbenzene</i>	41.2²	34.7	[46]	138 ± 45	[76,77]	8	[76,78]
<i>gasoline</i>	≈ 43	30.1–33.3	--	>95³	[44]	~23	
<i>Diesel fuel</i>	≈ 42	34.4–35.5	--	--	--	>51³	[45]

¹ LHV calculated from the enthalpy of formation (enthalpy of formation calculated with Joback's method [51]),

² LHV calculated from the enthalpy of combustion, ³Standardized value of ignition properties.

This is well shown in Figure 4 which plots RON vs boiling point for the five aromatic compounds, for which RON values were found (p-cresol (6 in Tables 1 to 3), anisole (8), 2-phenylethanol (18), 4-methylanisole (19) and 2,4-xylene (20)), as well as for some arenes (benzene (3), toluene (14), xylene isomers (28, 29, 30), ethylbenzene (31), and trimethylbenzene isomers (35, 36, 37)). This figure displays only a small common zone including trimethylbenzene isomers together with anisole and 4-methylanisole, the two most suitable molecules for an use as gasoline additives. 2-Phenylethanol has a boiling point just above the limit, with a RON of 116. As described in the coming part, these three compounds are the only ones, for which measurements of their ignition delay times or laminar flame velocities were published. For the other molecules with a boiling point below the limit no RON value was found. p-Cresol with a RON of 153 and 2,4-xylene with a RON of 140 have a boiling point below the limit, but a melting point close to room temperature.

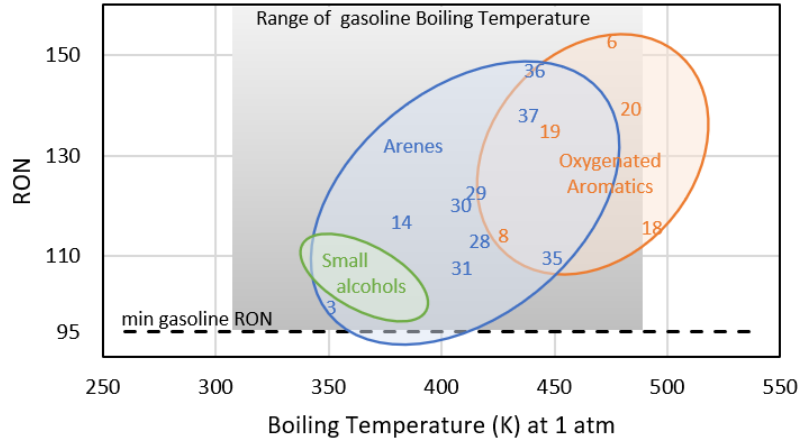
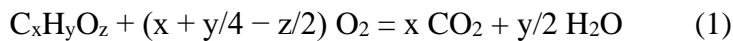


Figure 4: RON vs boiling points for the oxygenated aromatics, for which this value can be found, as well as of some arenes; the numbers are those of the species in Tables 1 to 3.

Concerning aromatic oxygenates used as additives in gasolines, Tian *et al.* have measured the RON value of mixtures made of a commercial (Dutch) Euro 95 gasoline and 10% of acetophenone, 2-phenylethanol and benzylalcohol [33]. RON values equal to 96.9, 96.9 and 96.1, respectively, were found confirming the octane boosting effect of adding aromatic oxygenates. McCormick *et al.* [34] measured the RON value for a base E0 gasoline (RON = 85.8) and its mixtures with 1% phenol, 2% p-cresol, 6% p-cresol, 2% xylenol, 2% guaiacol and 2% 4-methylguaiacol and found RON values equal to 86.7, 88.3, 91.9, 89.0, 86.2, and 86.4, respectively. The addition of all these phenolic compounds has a positive effect on RON, but problems due a limited solubility in gasoline were reported for phenol and cresol isomers.

3.2. Ignition delay times and laminar flame velocities

In addition to the numbers scaling the overall autoignition behavior of fuels as above described, two types of measurement targets are usually used to characterize fuel combustion: ignition delay times and laminar flame velocities. Table 5 presents the kinetic studies during which these data were measured for neat aromatic oxygenates. In the combustion studies involving such measurements, as well as in those with product quantification (see part 5), measurements are made under well-defined operating conditions, temperature (T), pressure (P) and reactive mixture composition. In such studies, an important parameter is the equivalence ratio (ϕ), which is defined for the global combustion reaction (1) of a $C_xH_yO_z$ fuel,



as $\phi = x_{fuel}/(x + y/4 - z/2)x_{O_2}$, with x_{fuel} and x_{O_2} , respectively the fuel and oxygen mole fractions.

In some cases, for facilitating kinetic experiments, helium or argon can be used as the diluent gas instead of nitrogen. In addition, to avoid too high temperature gradients due to reaction exothermicity, the ratio between the mole fraction of the diluent gas and that of oxygen is often

significantly higher than that for combustion in air (3.76). Above all, the physical models of the used experimental devices are simple enough to allow the simulation of the measured data using detailed kinetic models involving thousands of elementary reactions [85] by means of dedicated softwares, e.g. CHEMKIN [86], CANTERA [87], OPENSMOKE [88].

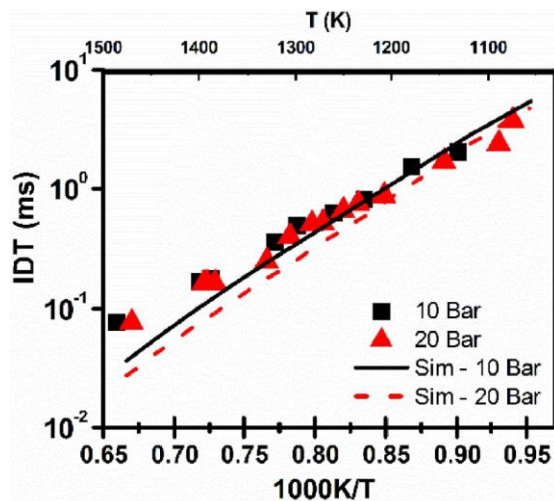
Table 6: Aromatic oxygenated kinetic studies, during which autoignition delays times or laminar flame velocities of neat aromatic oxygenates were measured.

Aromatic oxygenates studied	Instruments	Experimental Conditions	Reference
Measurement of ignition delay times			
anisole	Shock tube	$T_c=770-1600$ K; $P_c=10, 20, 40$ bar; $\Phi=0.5$	Herzler <i>et al.</i> , 2017 [89]
	RCM	$T_c=900-1315$ K; $P_c=10, 20, 40$ bar; $\Phi=0.5, 1$ $T_c=750-900$ K; $P_c=10, 20, 40$ bar; $\Phi=0.5, 1, 2$	Buttgen <i>et al.</i> , 2020 [57]
2-phenylethanol	Shock tube	$T_c=1050-1500$ K; $P_c=10, 20$ bar; $\Phi=0.5, 1$	Shankar <i>et al.</i> , 2017 [54]
	RCM	$T_c=813-992$ K; $P_c=10, 20, 30, 40$ bar; $\Phi=0.35, 0.5, 1, 1.5$	Fang <i>et al.</i> , 2021 [90]
Measurement of laminar flame velocity			
anisole	Bunsen burner	$T_i=423$ K, $P_i=1$ bar, $\Phi=0.6-1.3$	Wu <i>et al.</i> 2017 [75]
	PLF burner	$T_i=358$ K; $P_i=1$ bar; $\Phi=0.6-1.2$	Wagnon <i>et al.</i> , 2018 [91]
	Constant volume bomb	$T_i=460-575$ K; $P_i=1$ bar; $\Phi=0.8-1.4$ $T_i=460-575$ K; $P_i=0.5-3$ bar; $\Phi=1$	Zare <i>et al.</i> , 2019 [92]
4-methylanisole	Bunsen burner	$T_i=423$ K, $P_i=1$ bar, $\Phi=0.6-1.3$	Wu <i>et al.</i> 2017 [75]

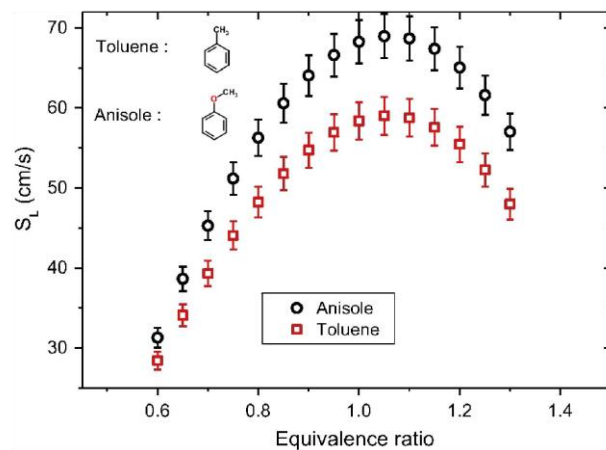
Index “*c*” is for parameters after compression and “*i*” for initial gas parameters.

3.2.1. Ignition delay times

Ignition delay times are usually measured using two types of devices, in which a reactive gas mixture is heated by compression. First, shock tubes, which are ideal totally adiabatic reactors, where a gas at low pressure is brought almost instantaneously to a known and controlled high temperature and pressure condition by means of the passage of a shock wave created by the sudden expansion of a high-pressure gas [93]. Second, rapid compression machines (RCM), in which the heating process of the gas mixture by mechanical compression is similar to that occurring during a single cycle of an internal combustion engine [94]. In both devices, the ignition delay time is the time between the moment, when the gas reaches the compressed temperature (T_c) and pressure (P_c), and the moment, when autoignition occurs as indicated by a sharp increase in pressure or radical emission [95]. As it is shown in Figure 5(a) for 2-phenylethanol, the obtained ignition delay times are usually plotted under logarithmic scale versus $1/T_c$ to check how the Arrhenius behavior is followed.



(a)



(b)

Figure 5: (a) Ignition delay times of 2-phenylethanol measured in a shock tube for $\phi = 1$ (symbols are measurements and lines simulations); (b) laminar flame velocities of anisole compared to those of toluene $T_b = 423$ K, P_b 1bar - reproduced from Refs. [54] and [75], respectively, with permission of Elsevier.

As it is shown in Table 6, there are only two aromatic oxygenates, for which measurements of ignition delay times of neat fuel can be found: anisole and 2-phenylethanol. These measurements were made in both shock tubes (undiluted fuel in air for anisole and highly diluted in argon for 2-phenylethanol) and RCMs (undiluted fuel in air or in a nitrogen/argon mixture). The results by Buttgen *et al.* [57] indicate an Arrhenius behavior under all their studied conditions with significantly higher slopes in RCM than in shock tube. Mergulhão *et al.* [96] also measured ignition delay times in a RCM for (40/60) anisole/iso-octane blend ($T_c = 684$ K, $P_c = 20$ bar, $\phi = 1$) and well showed a significant inhibiting effect of adding the aromatic oxygenate on the alkane reactivity.

3.2.2. Laminar flame velocities

As it is shown in Table 6, laminar flame velocities for aromatic oxygenates can only be found for anisole and 4-methylanisole. These measurements were performed using either a constant volume bomb, in which a flame is spark-ignited, or using flat flame or Bunsen burners; these methods were comprehensively described by Konnov *et al.* [97]. As shown in Figure 5(b), such measurements are usually plotted versus ϕ leading to a parabolic curve with a maximum for ϕ close to 1.1. The data displayed in Table 6 were obtained at atmospheric pressure, except the work of Zare *et al.* [92] performed from 0.5 to 3 bar. Temperatures (T_i) of the initial gases varied from 358 to 575 K. The first flame velocity measurements for aromatic oxygenates were published in 2017 by Wu *et al.* [75], who used OH chemiluminescence on a Bunsen burner. These authors studied neat anisole, 4-methylanisole and toluene reporting for $T_i = 423$ K

maximum value at $\phi = 1.06$ of 68.8, 65.6, and 58.1 cm/s, respectively. Later, Wagnon *et al.* used in a Premixed Laminar Flame (PLF) with the heat flux method [98] and Zare *et al.* [92] a constant volume bomb method for also measuring neat anisole flame velocity. However, as shown in Table 6, there is no common condition amongst the three sets of published data allowing data comparison.

3.3. Soot formation tendency

If change-of-state properties, global combustion parameters, and the emissions of gas phase pollutants are important factors for considering a molecule as a possible biofuel, this is also the case of its ability to produce soot. The Yield Sooting Index (YSI) indicates the relative tendency of different pure hydrocarbons to produce soot particulates under combustion conditions and can be measured by different combustion techniques as described by Das *et al.* [99]. Table 7 displays the YSI of various aromatic reactants according to the values given by [100].

Table 7: Experimental yield sooting index (YSI) of various aromatic reactants.

Aromatic oxygenates	YSI
catechol	34
p-guaiacol	55
o-guaiacol	64
o-guaiacol	64
3-methylanisole	103
anisole	111
2-ethylphenol	120
4-ethylphenol	128
3-ethylphenol	138
1-phenylethanol	142
<i>toluene</i>	<i>171</i>
<i>p-xylene</i>	<i>202</i>
<i>o-xylene</i>	<i>200</i>
ethylbenzene	222
m-xylene	216

Table 7 well shows that the aromatic oxygenates discussed in this paper have a lower sooting tendency than their non-oxygenated counterparts. However, aromatic oxygenates substituted by an alkyl groups such as ethylphenol show a higher sooting tendency than other aromatic oxygenates, such as anisole, despite the oxygen moiety. The lowest YSI are found for aromatic oxygenates including two O-atoms, i.e., catechol and guaiacol isomers.

4. Kinetics of combustion and the emissions from aromatic oxygenates

In this part, first the experimental studies are presented, then the detailed kinetic models, which have been developed to simulate these results, are described, and finally the influence of the structure of the aromatic compounds for the production of soot is discussed.

4.1. Experimental work

Since the beginning of the 80s, experiments on the pyrolysis of aromatic oxygenates providing product yields have been made using different types of batch reactors at atmospheric pressure, at temperatures from 678 to 1040 K and at residence times ranging from a few to several hundreds of minutes. This was the case of anisole studied by Schlosberg *et al.* [101], who reported phenol, methane and CO as the main products from their mass spectrometry (MS) analyses, and of o-guaiacol investigated by Ceylan and Bredenberg [102], who used a rocking autoclave using several co-reactants (e.g. H₂, tetralin, naphthalene...) and mostly reported the formation of phenol, o-cresol, catechol, methylcatechol, and methylguaiacol. Using gas chromatography (GC), Klein and co-workers [103,104] reported the formation of carbon monoxide, and methane to a lower extent, as major gaseous products from the pyrolysis of benzaldehyde, acetophenone, anisole and o-guaiacol. Liquid products included mainly benzene from benzaldehyde, o-cresol, phenol and benzene from anisole, catechol and phenol from o-guaiacol, and benzene, toluene, xylenes, from acetophenone. In respectively 1988 and 1999, Taylor *et al.* [105] and Chuchani *et al.* [106] were interested by the pyrolysis of 2-phenylethanol. Both teams observed the same major produced species, styrene and toluene, with ethylbenzene as a minor one; Taylor *et al.* [105], working at low pressure (0.086-0.263ba), also found traces of biphenyl, bibenzyl, 2-methoxyethylbenzene and 2-phenylethylether.

Table 8 presents the experimental studies using set-ups, which were not batch reactors and during which the species produced by the reaction (pyrolysis, oxidation, actual combustion) of monoaromatic oxygenates were quantified. This is only the case of C₆-C₈ compounds: phenol, catechol, benzaldehyde, anisole, benzyl alcohol, guaiacol isomers, and 2-phenylethanol isomers.

Table 8: Aromatic oxygenate kinetic works (pyrolysis, oxidation, actual combustion) made after 1980, during which reaction products were quantified.

Aromatic oxygenates	Experimental devices	Experimental Conditions	Reference
Phenol	Tubular reactor	T=1064-1162 K; P=1 atm; $\Phi=\infty$	Lovell <i>et al.</i> , 1989 [107]
		T=922-1175 K; P=1 atm; $\Phi=\infty$	Manion and Louw, 1989 [108]
	Shock tube	T=1450-1650 K; P=2.5 atm; $\Phi=\infty$	Horn <i>et al.</i> , 1998 [109]
		T=1170 K; P=1 atm; $\Phi=\infty$ -0.64-1.73	Brezinsky <i>et al.</i> , 1998 [110]
Catechol	Tubular reactor	T= 973,15- 1273 K, P=1 atm; $\Phi=\infty$	Ledesma <i>et al.</i> , 2002 [111]
		T= 773- 1273 K; P=1 atm ; $\Phi=0$ - 0.92	Thomas <i>et al.</i> , 2007 [112]
Benzaldehyde	JSR	T=700-1100K ; P = 1 atm, $\Phi=0.5$, 1, 2	Namysl <i>et al.</i> , 2020 [113]
		T=475–900 K ; P = 1 atm, $\Phi=0.4$, 2	Chen <i>et al.</i> , 2020 [114]
Anisole	Shock tube	T=1000-1580 K; P=0.4-0.9 atm; $\Phi=\infty$	Lin and Lin., 1986 [115]
		T= 1425, 1530 K; P= 1,60, 1.47 atm; $\Phi=\infty$	Zabeti <i>et al.</i> , 2017 [116]
	Tubular reactor	T=793-1020 K; P=1 atm; $\Phi=\infty$	Arends <i>et al.</i> , 1993 [117]
		T=999-1003 K; P=1 atm; $\Phi=\infty$, 1.05, 0.62, 1.71	Pecullan <i>et al.</i> , 1997 [118]
		T=1023-1173 K; $\Phi=\infty$	Platonov <i>et al.</i> , 2001 [119]
		T=873-1373 K; P=1 atm; $\Phi=\infty$	Friderichsen <i>et al.</i> , 2001 [120]
		T= 525-675 K ; P=1 atm; $\Phi=\infty$	Pelucchi <i>et al.</i> 2018 [121]
		T= 850-1160 K ; P= 0,04, 1 atm; $\Phi=\infty$	Yuan <i>et al.</i> 2018 [122]
		T=850-1000 K; P=0.015-0.12atm; $\Phi=\infty$	Mackie <i>et al.</i> , 1990 [123]
	JSR	T=673-1173 K; P=1 atm; $\Phi=\infty$, 1	Nowakowska <i>et al.</i> , 2014 [124]
		T=675-1275 K; P=1 atm; $\Phi=\infty$, 0.5, 1 and 2.	Wagnon <i>et al.</i> , 2018 [91]
	PLF burner	T _i =500 K; P _i =0.04 bar; $\Phi=1.2$, 1.6	Bierkandt <i>et al.</i> , 2019 [125]
	Laminar counterflow diffusion-flame burner	T _i =500 K; P _i =0.04 bar; $\Phi=1.2$, 1.6	Chen <i>et al.</i> , 2022 [126]
Benzyl alcohol	JSR	T=700–1100 K; P=1 atm; $\Phi=0.4$, and 2.0.	Zhou <i>et al.</i> , 2018 [127]
	Tubular reactor	T= 900–1275, 875–1223 ; K ; P=0.04, 1 atm; $\Phi=\infty$	Chen <i>et al.</i> , 2021 [128]
Guaiacol isomers	JSR	T=623-923 K; P=1 atm; $\Phi=\infty$, 1	Nowakowska <i>et al.</i> , 2018 [129]
	Micropyrolyser	T=623-823 K ; P=1 atm; $\Phi=\infty$	Yerrayya <i>et al.</i> , 2019 [130]
Phenyl ethanol isomers	Tubular reactor	T=800-1200 K; P = 1 bar, $\Phi=3$	Brian <i>et al.</i> , 2021 [131]
Ethylphenol isomers	Tubular reactor	T=900-1150 K; P = 1 bar, $\Phi=3$	Kim <i>et al.</i> , 2021 [100]

Index “_i” is for initial gas parameters.

Looking at the experimental devices listed in Table 8, those including a heated reactor, especially a flow reactor, were the most frequently used, with significantly less work made using shock tubes or flames. The usual flow reactors are either tubular reactors [132], which are simply tubes, through which reactive gases are flowing, or stirred reactors; typical residence times range from ~0.1 to ~10 s. Stirred flow reactors are mostly Jet-Stirred Reactors (JSRs), consisting of a sphere, in which four turbulent jets created from a cross-shaped inlet located at its center ensure the mixing [133]. Two studies, only about anisole, were made in flames, in a PLF and in a laminar counterflow diffusion-flame; more details about flame experiments can

be found in Egolfopoulos *et al.* [134]. The analysis method used with flow reactors was mainly GC, while flames were mostly investigated by MS.

4.1.1. Phenol

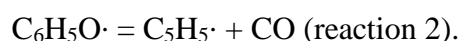
In addition to the kinetic studies listed in Table 8, in 1988, He *et al.* [135] performed experiments in a single-pulse shock tube over a range of temperatures from 1000 to 1150 K and pressures from 2.5 to 5 atm. They measured the rate constants of the hydrogen atom and hydroxyl radical attack on phenol (reaction 1) yielding the resonance stabilized phenoxy radical ($\text{C}_6\text{H}_5\text{O}\cdot$):



In the same way as for benzyl radical ($\text{C}_5\text{H}_5\text{CH}_2\cdot$) issued from toluene [136], the resonance stabilization of phenoxy radical promotes inhibiting reactions, such as combination with H-atoms or disproportionation with $\cdot\text{HO}_2$ radicals which consume radicals. The importance of such resonance stabilized radicals in the chemistry of aromatic compounds explain partly their high RON numbers.

The first study of the pyrolysis of phenol was performed in the group of Brezinsky [110] at Princeton (USA) using a tubular reactor at atmospheric pressure for temperatures between 1064 and 1162 K. Based on GC analyses, they identified the main pyrolysis products as being CO, cyclopentadiene and benzene. Manion and Louw [108] drew similar conclusions from their work on the phenol pyrolysis in H_2 using a similar reactor over a larger temperature range ($T = 922\text{--}1175$ K). Horn *et al.* [109] studied the pyrolysis of phenol in a shock tube at temperatures from 1450 to 1650 K using atomic and molecular resonance absorption spectroscopy as diagnostics. They deduced from their results that the main initiation reaction is the elimination of CO after an internal rearrangement of phenol.

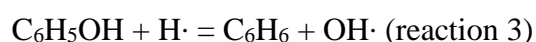
On line with their pyrolysis study, Brezinsky *et al.* [110] investigated the oxidation of phenol at atmospheric pressure near 1170 K over a range of equivalence ratios, 0.64–1.73. They found that cyclopentadiene was the major reaction intermediate and proposed its formation to occur through that of cyclopentadienyl radical ($\text{C}_5\text{H}_5\cdot$), which is produced from phenoxy radical via reaction (2):



This reaction is of particular importance, since for all aromatic hydrocarbons or oxygenates, it is the only pathway degrading the very stable benzene cycle. An important reaction of cyclopentadienyl radicals is the recombination with themselves yielding naphthalene [137] and

initiating the growth towards larger polyaromatic hydrocarbons (PAHs) and ultimately soot particulates [138].

Carbon monoxide, carbon dioxide, methane, acetylene, ethylene, 1,3-butadiene and benzene (obtained by ipso-addition of H-atoms, reaction 3) were the other observed major species quantified. Minor species included allene, methylacetylene, propene, ethane, methylcyclopentadiene, and naphthalene.

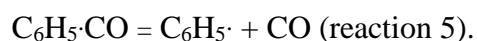


4.1.2. Catechol (also named pyrocatechol or ortho-dihydroxybenzene)

Because of the importance of this molecule for tobacco industry [139], a group in Louisiana State University has been interested by the kinetic studies of catechol. In 2002, they started a study of the pyrolysis of catechol in a tubular reactor ($T = 1273 \text{ K}$, $P = 1 \text{ atm}$) using high pressure liquid chromatography with ultraviolet-visible detection and identified 61 species, including many PAHs including more than three rings or ethenyl-substituted [139]. In a following work starting from 700 K and using GC, they quantified CO, methane, acetylene, ethylene, 1,3-butadiene, cyclopentadiene, benzene, phenol, and two- to eight-ring PAHs as the main products; minor ones included ethane, propyne, propadiene, and propylene. A third work [112] investigated ϕ ranging from ∞ (pure pyrolysis) to 1.08 (near stoichiometric oxidation) over a temperature range of 500–1000 K. Except CO_2 which was produced only during oxidation, similar products were formed whatever ϕ . CO, acetylene, benzene and 1,3-butadiene, are the major products. At a given temperature, the yield of 1,3-butadiene and that of PAHs, significantly increased when increasing ϕ . The authors concluded that 1,3-butadiene was a major intermediate in PAH formation under catechol pyrolysis and fuel-rich oxidation conditions [112].

4.1.3. Benzaldehyde

Benzaldehyde pyrolysis has been studied since 1929 [140–143]. These studies were mostly interested by the kinetics of the unimolecular decomposition leading to $\text{C}_6\text{H}_5\cdot\text{CO}$ radical (reaction 4), which decomposes yielding phenyl radical and CO through reaction (5):



Reaction 4 is favored due to the particularly low value of the dissociation energy of the broken C-H bond (373 kJ/mol, see figure 6). However, the $\text{C}_6\text{H}_5\cdot\text{CO}$ radical can also be easily obtained from benzaldehyde by H-abstraction.

Even no recent study presenting product quantification during benzaldehyde pyrolysis is available, in 2020, two papers reported results on the oxidation of benzaldehyde in JSRs, with 48 species quantified by GC [113] and 29 more by photo-ionization MS (at the National Synchrotron Radiation Laboratory in Hefei, China) [114]. Figure 6 shows the fuel consumption and the formation of the major products, CO, CO₂, and phenol as measured by GC. This important formation of carbon oxides and phenol supports the rapid formation of phenyl radicals by H-abstraction followed by reaction 5.

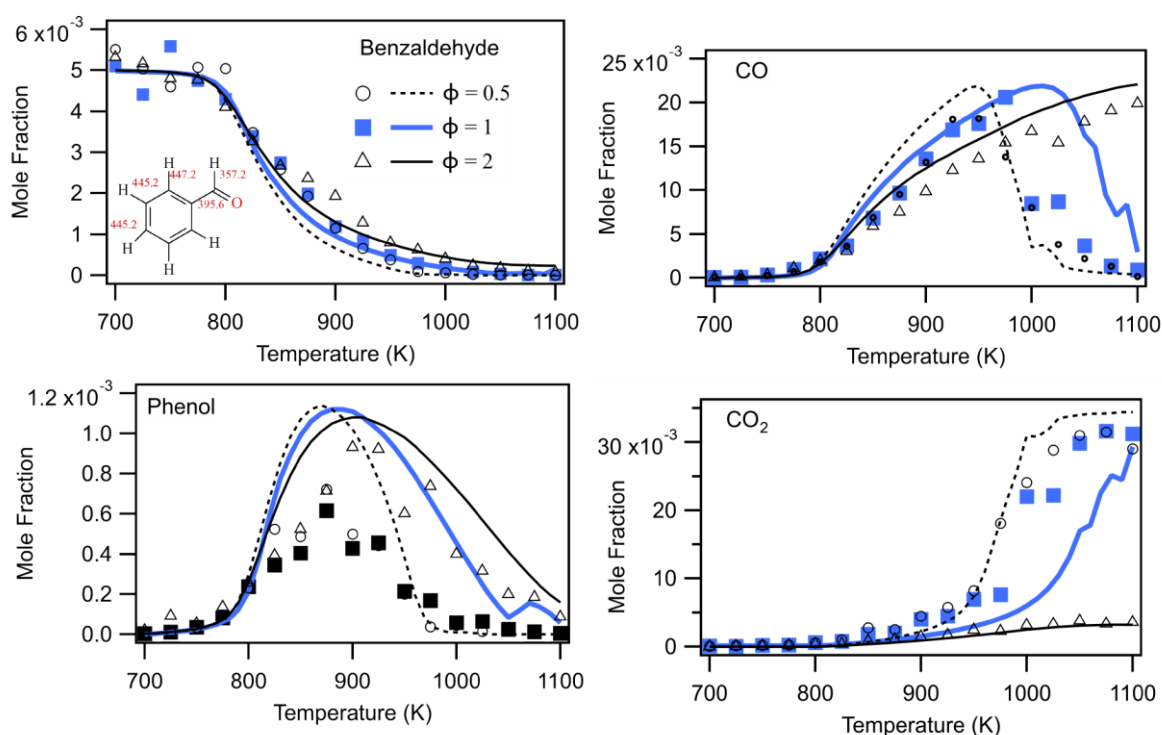
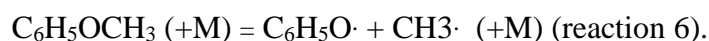


Figure 6: Oxidation of benzaldehyde in a JSR: Evolution with temperature of the mole fraction of fuel and major products, CO, CO₂, and phenol (symbols are experiments and lines computed data, for a residence time of 2 s) replotted from the data of [113]. The numbers near the bonds in the benzaldehyde molecule are bond dissociation energies in kJ/mol.

4.1.4. Anisole

Anisole is the aromatic oxygenate which has been the subject of the highest number of investigations starting from 1967 [144]. Two studies of anisole pyrolysis were performed behind shock waves. Lin and Lin [115] followed the formation of CO by laser resonance-absorption and derived from their measurements rate constants for related reactions, especially that of reactions (6) and (2); reaction (6) is significantly favored by the very low bond dissociation energy of the C-O bond connected to the methyl group (264.4 kJ/mol [124]):



These authors also proposed the possible formation of o- and p-cresol by reaction of methyl ($\text{CH}_3\cdot$) with phenoxy ($\text{C}_6\text{H}_5\text{O}\cdot$) radicals via methylcyclohexadienones. Zabeti *et al.* [116] used mass spectrometry to follow the time evolution of the mole fractions of anisole+cresol, $\text{CO}+\text{C}_2\text{H}_4$, and benzene.

Anisole pyrolysis was the most frequently investigated using flow reactors, with six studies in tubular reactors and three in JSRs. The studies in tubular reactors were started in 1993 by Arends *et al.* [117], who worked both in excess of hydrogen, quantifying methane and phenol as the major products, and in excess of fluorotoluene, proposing a rate constant for reaction (5). Later, Platonov *et al.* [119] showed using GC that increasing the temperature decreased the formation of phenolic compounds and increased that of PAHs. Friderichsen *et al.* [120] used both a flow reactor and a hyperthermal nozzle with time-of-flight mass spectrometry and Fourier transform infrared spectroscopy. From the identification of free radicals and reaction intermediates, they demonstrated the importance of phenoxy and cyclopentadienyl radicals in the formation of naphthalene. More recently, Pelucchi *et al.* [121] reported, as is shown in Figure 7, a wide range of stable products including bicyclic aromatics, such as benzofuran. The main quantified products were methane, carbon monoxide, phenol and benzaldehyde. Using photo-ionization MS (at the National Synchrotron Radiation Laboratory in Hefei, China), Yuan *et al.* [122] achieved the most comprehensive speciation including the previously reported stable products, but also, radicals, especially the three key ones for anisole pyrolysis, $\text{C}_6\text{H}_5\text{O}\cdot$, $\text{C}_5\text{H}_5\cdot$ and $\text{CH}_3\cdot$ radicals.

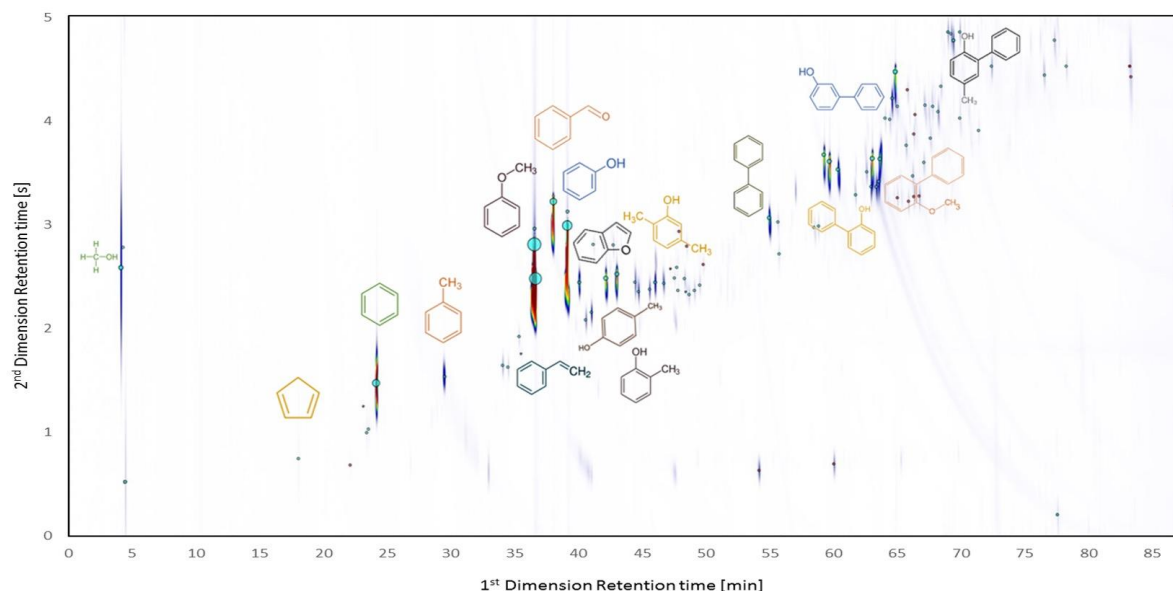


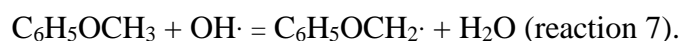
Figure 7: Pyrolysis of anisole in a flow reactor: chromatogram obtained by 2-dimension GC with flame ionization detection for a reactor temperature of 848 K [121] – Figure provided by the authors.

To finish with tubular reactor studies, the 1997 study by Pecullan *et al.* [118] in the group of Brezinsky was the first one investigating both the pyrolysis and the oxidation of anisole. The experiments demonstrated anisole thermal decomposition near 1000 K to proceed only through reaction (5). Using GC, the same major products, i.e., phenol, cresols, methylcyclopentadiene, and CO, were quantified both during pyrolysis and oxidation.

Concerning studies in a stirred reactor. In 1989, Mackie *et al.* [123] used a perfectly stirred reactor with a geometry different from the JSRs used nowadays and worked at pressure significantly below 1 atm. Using GC, they concluded CO, phenol and cresols to be the most important products from anisole pyrolysis. More recently, the pyrolysis of anisole and its oxidation were studied in JSRs using GC for product quantification by Nowakowska *et al.* [124] in Nancy and by Wagnon *et al.* [145] in Orléans. Both studies agreed on the important formation of carbon monoxide, 1,3-cyclopentadiene, benzene, phenol and cresol as the major reaction products, these products being the same for pyrolysis and oxidation.

Two recent studies focused on the quantification of products in anisole flames. Using photoionization MS (at the Advanced Light Source in Berkeley, USA, and at the Swiss Light Source in Villigen, Switzerland) with photoelectron spectroscopy, Bierkandt *et al.* [125] reported the quantification of more than 60 species in PLF. In addition to CO and H₂, CH₃· radical, CH₄, C₂H₂, C₂H₄, C₂H₆, CH₂O, C₅H₅· radical, cyclopentadiene, benzene, phenol, and benzaldehyde were the intermediates produced in the highest amounts, with mole fractions of the order of 10⁻³–10⁻²; phenoxy radical was measured with mole fractions up to 10⁻⁴. Time-of-flight molecular-beam MS and GC were used by Chen *et al.* to investigate a laminar counterflow diffusion-flame of anisole under oxy-fuel conditions [126]. Forty stable species, including naphthalene and dibenzofuran, were reported.

In parallel of their measurements of ignition delay times in a RCM for an anisole/isooctane blend, Mergulhão *et al.* [96] also followed the time evolution of the both reactants and several products, including three aromatic species, benzene, toluene and benzaldehyde. Under those low-temperature conditions, anisole reacts mainly by abstraction of H-atom on the methyl group (reaction 7) to give anisyl (C₆H₅OCH₂·) radical, which mainly adds to oxygen and leads cyclohexadienone or phenol, and for the major part to a non-cyclic C₅ species:



4.1.5. Benzyl alcohol

Only two kinetic studies were found concerning benzyl alcohol. Chen *et al.* [128] investigated its pyrolysis working in a tubular reactor using photo-ionization MS (at the National Synchrotron Radiation Laboratory in Hefei, China). They quantified 35 intermediates and products including C₁-C₅ species, monophenyl ring species, and a large number of PAHs. The monophenyl ring species are mainly benzene produced by ipso-addition of H-atom, benzyl (C₆H₅CH₂·) radical yielded by the fuel unimolecular decomposition, toluene deriving from benzyl radical, phenol and benzaldehyde, which arise mostly from the abstraction of the benzylic H-atom (reaction 8) followed by an H-elimination,



Zhou *et al.* [127] studied benzyl alcohol oxidation in a JSR with GC analysis. Major quantified products were CO, benzene, benzaldehyde; minor ones included methane, ethane, acetaldehyde, phenol, and benzofuran.

4.1.6. Guaiacol isomers (also named methoxyphenol isomers)

In 2011, Scheer *et al.* [146] used a heated SiC micro tubular (μ -tubular) reactor to investigate the pyrolysis of the three isomers of guaiacol. The decomposition products were identified by both laser photoionization time-of-flight MS using a laser and infrared spectroscopy. It was established that for the three isomers the initial step (reaction 9) is the loss of a methyl group, as it was previously described for anisole,



The OHC₆H₅O· radical decomposes to give CO and cyclopentadione, which can lose again CO to yield acetylene and vinylacetylene. The presence of phenol was also reported.

More recently, the pyrolysis and the oxidation under stoichiometric conditions of o-guaiacol was studied by Nowakowska *et al.* [129] in a JSR. As is shown by Figure 8, the presence of oxygen only slightly enhances the reactivity of both fuels, but the temperature where 50% of fuel consumed is about 100 K lower for guaiacol than for anisole. This earlier decomposition of guaiacol is due to the weakness of the O—CH₃ bond, whose dissociation energy drops from 274.5 kJ/mol in anisole to 243.1 kJ/mol in guaiacol.

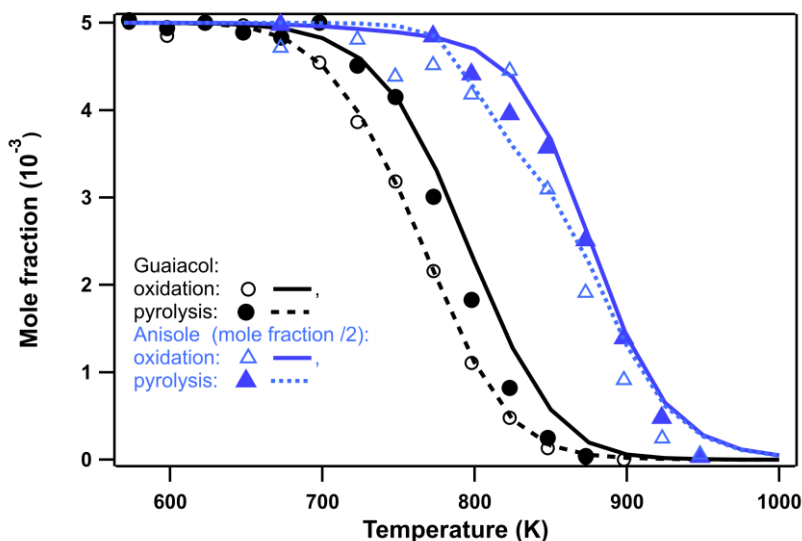


Figure 8: Comparison between the guaiacol and anisole results of Nowakowska [119, 100]: symbols are experimental fuel mole fractions, full symbols for pyrolysis and empty ones for oxidation, lines are simulations using the model of [119].

During the JSR work of [129], 22 species were quantified in pyrolysis and 42 in oxidation, the main common ones (maximum mole fraction $> 1\%$ of the fuel initial mole fraction) being CO, methane, ethane ethylene, 1,3-butadiene, 1,3-cyclopentadiene and phenolic molecules, such as phenol, catechol, 2-hydroxybenzaldehyde and methylcatechol. Catechol and methylcatechols arise from the $\text{OHC}_6\text{H}_5\text{O}\cdot$ radical obtained by unimolecular decomposition; the $\text{OHC}_6\text{H}_5\text{OCH}_2\cdot$ radical obtained by H-abstraction from the methyl group was considered to lead mainly to 2-hydroxybenzaldehyde.

After that, the fast pyrolysis of o-guaiacol was investigated by Yerrayya *et al.* [130] using a micropyrolyzer consisting of a quartz tube inside a pre-heated furnace into which the sample taken in a deactivated stainless steel cup was dropped. Thanks to GC analyses, 42 products were quantified, the major ones being phenol, o-hydroxybenzaldehyde, catechol, and o-cresol.

4.1.7. Phenylethanol isomers

In 2017, Singh *et al.* [147] used a shock tube with GC coupled with MS to identify benzene, toluene and styrene as the major products of 2-phenyl-ethanol pyrolysis. Ethylbenzene and phenylacetylene were found in smaller quantities and benzaldehyde observed as traces.

In 2021, NREL researchers in Golden (USA) [131] investigated the oxidation 1- and 2-phenylethanol in a tubular reactor using GC. As they were mostly interested by soot tendency, the authors worked at $\phi = 3$, an equivalence ratio chosen to simulate the fuel rich zones of a

Diesel spray, in which both pyrolysis and combustion occur. They found carbon monoxide, benzene, toluene, styrene and benzaldehyde to be the main products; the formation of acetophenone was also reported for 1-phenyl-ethanol and that of phenylacetaldehyde (PHAL) for 2-phenyl-ethanol. Figure 9 shows the main reaction pathways proposed by Brian *et al.* [131] for 2-phenylethanol with the energies they calculated for the related transition states to explain the formation of these products.

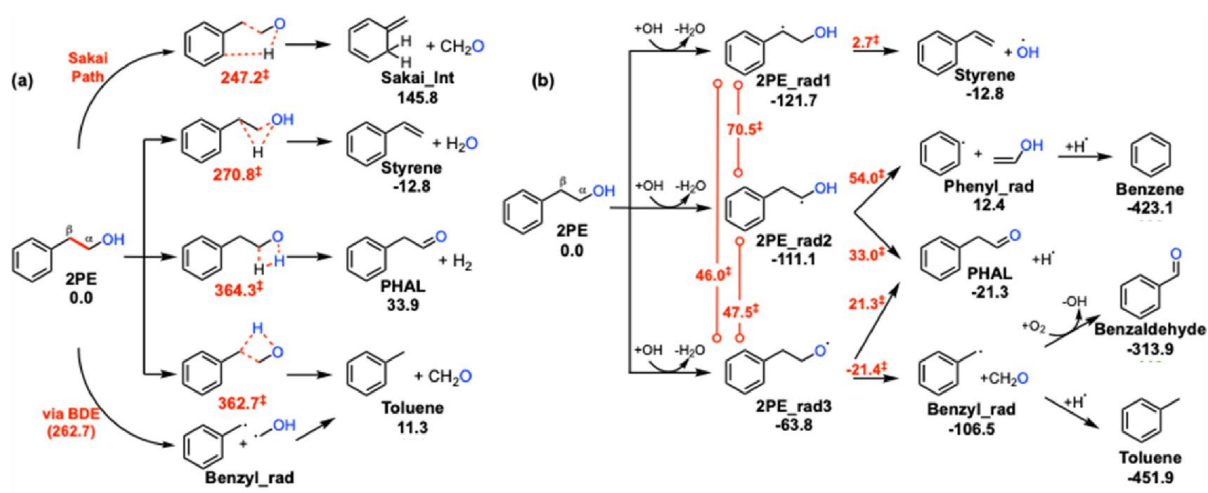


Figure 9: Major reactions pathways of 2-phenyl ethanol proposed by [131]: (a) unimolecular reactions, (b) reactions starting by an H-abstraction (red dotted lines show bond breaking and forming in transition state structures, red values are activation energy barriers and black values are product energies; all energies are computed using the composite G4 theory (kJ/mol) – reproduced from [131] with the permission of Elsevier.

4.1.8. Ethylphenol isomers

NREL researchers in Golden (USA) [100] used the same experimental method as for phenylethanol isomers to study the oxidation of 2-ethylphenol and 3-ethylphenol. While phenylethanol isomers were fully consumed since 1020 K, this was only the case from 1075 K for 2-ethylphenol and from 1150 K for 3-ethylphenol. Carbon monoxide, methane, ethylene, ethane, benzene, toluene, styrene were found to be the major products at 1150 K for both reactants, as well as naphthalene and benzofuran from 2-ethylphenol, and cyclopentadiene and dihydrobenzofuran from 3-ethylphenol. At 1000 K, 2-ethylphenol produces more oxygenated products (phenol, 2-methylphenol, 2-methylbenzaldehyde) than 3-ethylphenol since the ortho position favors resonance stabilization of radical intermediates.

4.1.9. Phenyl acetate

Concerning phenyl rings substituted by an ester function, there is no kinetic studies up to now presenting product quantification during the pyrolysis or the oxidation of these molecules. However, two studies focused on the measurement of the rate constant the decomposition of phenyl acetate (reaction 10) yielding phenol and ketene through a four-center transition state (see [105,148]):



4.2. Proposed detailed kinetic models for aromatic oxygenates

As shown in Table 8, which lists the major kinetic models developed for aromatic oxygenates, since 1986 with study on anisole by Lin and Lin [110], the modelling of the combustion of aromatic oxygenates have been progressing as far as experimental data were made available as detailed in part 4.1. When several versions of a model have been developed successively, only the last updated version is listed. Because of the large amount of studies on anisole, many models were developed and validated for this reactant.

Table 8: Major detailed kinetic models validated against experimental results developed for aromatic oxygenates.

Kinetic model 1st author, year, reference	Reactions/ species	Phenol	Catechol	Benzal dehyde	Anisole	Cresol	Benzyl alcohol	Benzo furan	Guaiacol	Phenyl ethanol
Lin 1986 [115]	10/15			+	V	+				
Arends 1993 [117]	37/23	+		+	V	+				
Pecullan 1997 [118]	66/31	+		+	V	+				
Horn 1998 [109]	18/21	V								
Shankar 2017 [54]	2911/548	+		+		+	+			V
Nowakowska 2018 [129]	1601/233	+	+	+	V	+	+	+	V	
Yuan 2019 [122]	2563/432	+	+	+	V	+	+	+	+	
Buttgen 2020 [57]	2757/484	+		+	V	+	+	+		
Pratali Meffei 2020 [149]	14332/368	V	V	V	V	+	+	+	V	
Mergulhão 2021 [95]	9998/2368	+	+	+	V	+	+	+	+	
Chen 2021 [128]	2171/376	+		V		+	V	+		

V: species, for which the model, or a previous version was validated

+: species only present in the mechanism.

A few small size pyrolysis models were developed up to 1998. Lin and Lin [115] proposed a kinetic model for anisole, which was validated against the CO production profiles that these authors measured in a shock tube and which includes only 10 reactions considering the formation of cresols and benzaldehyde. This model was followed by larger ones taking into account the formation of phenol by Arends *et al.* [117] and Pecullan *et al.* [118] and validated against experimental data obtained in tubular reactors by the respective authors. In 1998, Horn *et al.* [109] developed the first model for phenol considering 18 reactions and 21 species and validated it using their shock tube H- and CO-concentration profiles.

In 2017, the group of Sarathy at KAUST [54] developed a kinetic model for 2-phenylethanol oxidation including 2911 reactions and reproducing well the Ignition Delay Times (IDTs) measured by the authors in a shock tube, but also those obtained later by [89] in a Rapid compression Machine (RCM). This work revealed the importance of reactions related to phenol in the oxidation of anisole and the need of considering O₂ addition pathways to explain the higher reactivity of 2-phenylethanol at low-temperature.

After 2017, due to an increased interest for molecules derived from biomass, several detailed kinetic models including several thousands of elementary reactions were developed for the pyrolysis, but also the oxidation and combustion of anisole. Nowakowska *et al.* [119] developed a detailed kinetic model for anisole oxidation, with an upgraded version for guaiacol, which considered a large number of aromatic oxygenates and was validated against the authors JSR quantifications [124,129]. Yuan *et al.* [122] adapted their model for the oxidation of small arenes (toluene, styrene, and ethylbenzene) to propose a model for anisole validated against their quantification in a tubular reactor for pyrolysis, as well as against literature data of anisole combustion, including IDTs in a shock tube [89], and speciation profiles in a tubular reactor [118], in two JSRs [91][119] and in laminar flame [125]. Büttgen *et al.* [57] extended the toluene mechanism developed in Galway [150] to anisole with validation against their shock tube and RCM IDTs, as well as against JSR speciation data by [119] and [90]. Updating the anisole model developed by Wagnon *et al.* [91], which was validated against their laminar flame velocity measurements and against JSR speciation data from their own and from [119], Mergulhão *et al.* [96] proposed an iso-octane/anisole model to simulate the influence of anisole addition on the IDTs of the alkane in RCM.

Apart anisole, kinetic models are available for only a few aromatic oxygenates. Chen *et al.* [128] published a detailed model of benzylalcohol oxidation, which was validated against the JSR data of the own authors, as well as against JSR data for benzaldehyde [113,114]. Ning *et al.* [151] reported a kinetic model of phenyl formate pyrolysis, but without attempt of validation using experimental data. This model indicates that the unimolecular decomposition reactions of phenyl formate to produce phenol + CO and 2,4-cyclohexadienone + CO are the dominant

decomposition pathways. No validated model can be found for cresol isomers or benzofuran, however, using their automatic generator of detailed kinetic model, the team of Green at MIT [138] develop kinetic models for the oxidation of p-cresol, m-cresol, o-cresol, 2,4-xyleneol, 2-ethylphenol, and guaiacol, but with as only validation comparison with their anti-knock tendency.

Validated kinetic models for the widest range of aromatic oxygenates were developed at Politecnico di Milano. Due to the long interest of the team of Ranzi and Faravelli in modelling biomass pyrolysis [152], the kinetic mechanisms of the pyrolysis, oxidation and combustion of gas, liquid and solids, so-called CRECK mechanism, [149] has considered since long aromatic oxygenates. This model based on lumped reaction was validated against literature experimental results obtained for:

- phenol [149], H- and CO-concentration profiles obtained in a shock tube by Horn *et al.* and measurements in tubular reactor by Brezinsky *et al.* [106] and Manion and Louw [104],
- catechol, mole fractions in tubular reactor [108],
- benzaldehyde, JSR mole fractions [113],
- anisole [153], mole fractions in JSR [91] and tubular reactor [116] and shock tube data [111]
- o-guaiacol, product quantification during guaiacol pyrolysis in a static reactor at 656 K [104].

Conclusion and perspectives

Lignin is a still underexploited part of lignocellulose, for which an increasing number of catalytic processes are proposed in order to produce molecules considered as potential components of biofuels. Those molecules are mainly substituted aromatics, including arenes with large number possible substitutions, but also compounds including one or two oxygenated functional groups, i.e. aromatic oxygenates. In order to tailor the most suitable molecules for using in combustion processes, this paper has inspected several relevant **properties of aromatic oxygenates**. The main conclusion reached are:

1. An important drawback of aromatic oxygenates for being used in combustion processes is their significantly **lower volatility** compared to arenes containing the same number of carbon atoms; some small aromatic oxygenates are even solid at room temperature (e.g., phenol).
2. Another notable drawback of this class of compounds is their **low LHVs** due the presence of oxygen atoms.
3. Despite RON values can only be found for a few aromatic oxygenates, the **high RON values** (above 100) of most of the aromatic oxygenates would make them suitable octane boosters in gasoline. However, due to the volatility issues, amongst the oxygenated ones, only anisole, acetophenone, 4-methylanisole, and to lesser extent p-

cresol, 2,4-xylenol and 2-phenylethanol, can really be considered as gasoline additives. In contrast, their low CN values make aromatic oxygenates difficult to be considered in Diesel fuels.

4. Certainly due to volatility issues, **measurements could only be found about the autoignition delay times of anisole and 2-phenylethanol and about the laminar flame velocities of anisole and 4-methylanisole.** The laminar flame velocity of anisole is about 15% larger than that of toluene.
5. A notable advantage of using aromatic oxygenates in combustion processes is their **lower tendency to form soot.**
6. **The majority of the experimental kinetic studies involving product quantification are related to pyrolysis, with carbon monoxide always being the major product.** No such work can be found for cresol isomers, 4-methylanisole and acetophenone. However, due to the importance of unimolecular reactions, a large part of reaction channels and products are common between pyrolysis and oxidation conditions with a large production of aromatic hydrocarbons and PAHs and a significant influence of the structure of the reactant. Aromatic resonance-stabilized radicals, such as phenoxy and benzyl radicals play an important role in the involved chemistry.
7. **highly validated detailed kinetic models can be found for anisole, but it is less the case for other aromatic oxygenates.** Since no experimental data are available, no validated model can be found for cresol isomers.

Another class of compounds which could be catalytically derived from lignin by pushing further the hydrogenation of the aromatic ring in arenes is substituted cyclohexanes. These non-aromatic cyclic compounds have a higher volatility than aromatic oxygenates, with a lower tendency to form soot than arenes, and much higher LHVs.

This article is a preliminary literature analysis of the fuel performance and related research of the oxygenated aromatic products of the CLS reaction. We expect in the near future to be able to give a clearer elucidation of the combustion performance of such molecules as the progress of the research. With such efforts we contribute to the optimization and upgrading of the products of the CLS reactions.

Acknowledgement

This work has received funding from the European Union's Horizon 2020 research and innovation program, (BUILDING A LOW-CARBON, CLIMATE RESILIENT FUTURE: SECURE, CLEAN AND EFFICIENT ENERGY) under Grant Agreement No 101006744. The content presented in this document represents the views of the authors, and the European Commission has no liability in respect of the content.

REFERENCES

- [1] A. Gómez-Barea, B. Leckner, Modeling of biomass gasification in fluidized bed, *Progress in Energy and Combustion Science*. 36 (2010) 444–509. <https://doi.org/10.1016/j.pecs.2009.12.002>.
- [2] S. Xiu, A. Shahbazi, Bio-oil production and upgrading research: A review, *Renewable and Sustainable Energy Reviews*. 16 (2012) 4406–4414. <https://doi.org/10.1016/j.rser.2012.04.028>.
- [3] G.W. Huber, S. Iborra, A. Corma, Synthesis of Transportation Fuels from Biomass: Chemistry, Catalysts, and Engineering, *Chem. Rev.* 106 (2006) 4044–4098. <https://doi.org/10.1021/cr068360d>.
- [4] Z. Wang, K.G. Burra, T. Lei, A.K. Gupta, Co-pyrolysis of waste plastic and solid biomass for synergistic production of biofuels and chemicals-A review, *Progress in Energy and Combustion Science*. 84 (2021) 100899. <https://doi.org/10.1016/j.pecs.2020.100899>.
- [5] Z. Sun, B. Fridrich, A. de Santi, S. Elangovan, K. Barta, Bright Side of Lignin Depolymerization: Toward New Platform Chemicals, *Chem. Rev.* 118 (2018) 614–678. <https://doi.org/10.1021/acs.chemrev.7b00588>.
- [6] F. Yan, R. Ma, X. Ma, K. Cui, K. Wu, M. Chen, Y. Li, Ethanolysis of Kraft lignin to platform chemicals on a MoCl₃-x/Cu-MgAlO₃ catalyst, *Applied Catalysis B: Environmental*. 202 (2017) 305–313. <https://doi.org/10.1016/j.apcatb.2016.09.030>.
- [7] Y. Román-Leshkov, C.J. Barrett, Z.Y. Liu, J.A. Dumesic, Production of dimethylfuran for liquid fuels from biomass-derived carbohydrates, *Nature*. 447 (2007) 982–985. <https://doi.org/10.1038/nature05923>.
- [8] J.S. Luterbacher, D. Martin Alonso, J.A. Dumesic, Targeted chemical upgrading of lignocellulosic biomass to platform molecules, *Green Chem.* 16 (2014) 4816–4838. <https://doi.org/10.1039/C4GC01160K>.
- [9] W. Leitner, J. Klankermayer, S. Pischinger, H. Pitsch, K. Kohse-Höinghaus, Advanced Biofuels and Beyond: Chemistry Solutions for Propulsion and Production, *Angewandte Chemie International Edition*. 56 (2017) 5412–5452. <https://doi.org/10.1002/anie.201607257>.
- [10] J.C. Guibet, *Fuels and Engines*, TECHNIP, 1997.
- [11] C. Li, X. Zhao, A. Wang, G.W. Huber, T. Zhang, Catalytic Transformation of Lignin for the Production of Chemicals and Fuels, *Chem. Rev.* 115 (2015) 11559–11624. <https://doi.org/10.1021/acs.chemrev.5b00155>.
- [12] J.-P. Lange, Lignocellulose conversion: an introduction to chemistry, process and economics, *Biofuels, Bioproducts and Biorefining*. 1 (2007) 39–48. <https://doi.org/10.1002/bbb.7>.

- [13] W. Schutyser, T. Renders, S. Van den Bosch, S.-F. Koelewijn, G.T. Beckham, B.F. Sels, Chemicals from lignin: an interplay of lignocellulose fractionation, depolymerisation, and upgrading, *Chem. Soc. Rev.* 47 (2018) 852–908. <https://doi.org/10.1039/C7CS00566K>.
- [14] X. Ma, R. Ma, W. Hao, M. Chen, F. Yan, K. Cui, Y. Tian, Y. Li, Common Pathways in Ethanolysis of Kraft Lignin to Platform Chemicals over Molybdenum-Based Catalysts, *ACS Catal.* 5 (2015) 4803–4813. <https://doi.org/10.1021/acscatal.5b01159>.
- [15] B. Güvenatam, E.H.J. Heeres, E.A. Pidko, E.J.M. Hensen, Lewis-acid catalyzed depolymerization of Protobind lignin in supercritical water and ethanol, *Catalysis Today*. 259 (2016) 460–466. <https://doi.org/10.1016/j.cattod.2015.03.041>.
- [16] J.B. Nielsen, A. Jensen, C.B. Schandel, C. Felby, A.D. Jensen, Solvent consumption in non-catalytic alcohol solvolysis of biorefinery lignin, *Sustainable Energy Fuels*. 1 (2017) 2006–2015. <https://doi.org/10.1039/C7SE00381A>.
- [17] A. Riaz, D. Verma, H. Zeb, J.H. Lee, J.C. Kim, S.K. Kwak, J. Kim, Solvothermal liquefaction of alkali lignin to obtain a high yield of aromatic monomers while suppressing solvent consumption, *Green Chem.* 20 (2018) 4957–4974. <https://doi.org/10.1039/C8GC02460J>.
- [18] K. Barta, T.D. Matson, M.L. Fettig, S.L. Scott, A.V. Iretskii, P.C. Ford, Catalytic disassembly of an organosolv lignin via hydrogen transfer from supercritical methanol, *Green Chem.* 12 (2010) 1640–1647. <https://doi.org/10.1039/C0GC00181C>.
- [19] Q. Song, F. Wang, J. Cai, Y. Wang, J. Zhang, W. Yu, J. Xu, Lignin depolymerization (LDP) in alcohol over nickel-based catalysts via a fragmentation–hydrogenolysis process, *Energy Environ. Sci.* 6 (2013) 994. <https://doi.org/10.1039/c2ee23741e>.
- [20] P. Ferrini, R. Rinaldi, Catalytic Biorefining of Plant Biomass to Non-Pyrolytic Lignin Bio-Oil and Carbohydrates through Hydrogen Transfer Reactions, *Angewandte Chemie International Edition*. 53 (2014) 8634–8639. <https://doi.org/10.1002/anie.201403747>.
- [21] X. Huang, T.I. Korányi, M.D. Boot, E.J.M. Hensen, Catalytic Depolymerization of Lignin in Supercritical Ethanol, *ChemSusChem*. 7 (2014) 2276–2288. <https://doi.org/10.1002/cssc.201402094>.
- [22] R. Ma, W. Hao, X. Ma, Y. Tian, Y. Li, Catalytic Ethanolysis of Kraft Lignin into High-Value Small-Molecular Chemicals over a Nanostructured α -Molybdenum Carbide Catalyst, *Angewandte Chemie International Edition*. 53 (2014) 7310–7315. <https://doi.org/10.1002/anie.201402752>.
- [23] X. Huang, T.I. Korányi, M.D. Boot, E.J.M. Hensen, Ethanol as capping agent and formaldehyde scavenger for efficient depolymerization of lignin to aromatics, *Green Chem.* 17 (2015) 4941–4950. <https://doi.org/10.1039/C5GC01120E>.
- [24] X. Huang, T.I. Korányi, M.D. Boot, E.J.M. Hensen, Catalytic Depolymerization of Lignin in Supercritical Ethanol, *ChemSusChem*. 7 (2014) 2276–2288. <https://doi.org/10.1002/cssc.201402094>.

- [25] F. Mai, Z. Wen, Y. Bai, Z. Ma, K. Cui, K. Wu, F. Yan, H. Chen, Y. Li, Selective Conversion of Enzymatic Hydrolysis Lignin into Alkylphenols in Supercritical Ethanol over a $\text{WO}_3/\gamma\text{-Al}_2\text{O}_3$ Catalyst, *Ind. Eng. Chem. Res.* 58 (2019) 10255–10263. <https://doi.org/10.1021/acs.iecr.9b01593>.
- [26] L.-P. Xiao, S. Wang, H. Li, Z. Li, Z.-J. Shi, L. Xiao, R.-C. Sun, Y. Fang, G. Song, Catalytic Hydrogenolysis of Lignins into Phenolic Compounds over Carbon Nanotube Supported Molybdenum Oxide, *ACS Catal.* 7 (2017) 7535–7542. <https://doi.org/10.1021/acscatal.7b02563>.
- [27] Y. Sang, K. Wu, Q. Liu, Y. Bai, H. Chen, Y. Li, Catalytic Ethanolysis of Enzymatic Hydrolysis Lignin over an Unsupported Nickel Catalyst: The Effect of Reaction Conditions, *Energy Fuels.* 35 (2021) 519–528. <https://doi.org/10.1021/acs.energyfuels.0c02848>.
- [28] Y. Sang, M. Chen, F. Yan, K. Wu, Y. Bai, Q. Liu, H. Chen, Y. Li, Catalytic Depolymerization of Enzymatic Hydrolysis Lignin into Monomers over an Unsupported Nickel Catalyst in Supercritical Ethanol, *Ind. Eng. Chem. Res.* 59 (2020) 7466–7474. <https://doi.org/10.1021/acs.iecr.0c00812>.
- [29] Y. Jing, L. Dong, Y. Guo, X. Liu, Y. Wang, Chemicals from Lignin: A Review of Catalytic Conversion Involving Hydrogen, *ChemSusChem.* 13 (2020) 4181–4198. <https://doi.org/10.1002/cssc.201903174>.
- [30] J. Kong, M. He, J.A. Lercher, C. Zhao, Direct production of naphthenes and paraffins from lignin, *Chem. Commun.* 51 (2015) 17580–17583. <https://doi.org/10.1039/C5CC06828B>.
- [31] Y. Bai, K. Cui, Y. Sang, K. Wu, F. Yan, F. Mai, Z. Ma, Z. Wen, H. Chen, M. Chen, Y. Li, Catalytic Depolymerization of a Lignin-Rich Corncob Residue into Aromatics in Supercritical Ethanol over an Alumina-Supported NiMo Alloy Catalyst, *Energy Fuels.* 33 (2019) 8657–8665. <https://doi.org/10.1021/acs.energyfuels.9b01457>.
- [32] Q. Liu, Y. Bai, H. Chen, M. Chen, Y. Sang, K. Wu, Z. Ma, Y. Ma, Y. Li, Catalytic conversion of enzymatic hydrolysis lignin into cycloalkanes over a gamma-alumina supported nickel molybdenum alloy catalyst, *Bioresource Technology.* 323 (2021) 124634. <https://doi.org/10.1016/j.biortech.2020.124634>.
- [33] M. Tian, R. Van Haaren, J. Reijnders, M. Boot, Lignin Derivatives as Potential Octane Boosters, SAE International. (2015).
- [34] R.L. McCormick, M.A. Ratcliff, E. Christensen, L. Fouts, J. Luecke, G.M. Chupka, J. Yanowitz, M. Tian, M. Boot, Properties of Oxygenates Found in Upgraded Biomass Pyrolysis Oil as Components of Spark and Compression Ignition Engine Fuels, *Energy Fuels.* 29 (2015) 2453–2461. <https://doi.org/10.1021/ef502893g>.
- [35] Fluidat, (n.d.). <https://www.fluidat.com/default.asp> (accessed September 28, 2021).
- [36] Gouvernement du Canada, Rapport d'évaluation préalable pour le Défi Pyrocatéchol (Catéchol). Numéro de registre du Chemical Abstracts Service 120-80-9. Environnement

- Canada-Santé Canada, (2008). <https://www.ec.gc.ca/ese-ees/default.asp?lang=Fr&n=04FDC10E-1#a4> (accessed September 28, 2021).
- [37] J. Biet, M.H. Hakka, V. Warth, P.-A. Glaude, F. Battin-Leclerc, Experimental and Modeling Study of the Low-Temperature Oxidation of Large Alkanes, *Energ. Fuel.* 22 (2008) 2258–2269. <https://doi.org/10.1021/ef8000746>.
- [38] M. Tian, R.L. McCormick, M.A. Ratcliff, J. Luecke, J. Yanowitz, P.-A. Glaude, M. Cuijpers, M.D. Boot, Performance of lignin derived compounds as octane boosters, *Fuel.* 189 (2017) 284–292. <https://doi.org/10.1016/j.fuel.2016.10.084>.
- [39] Merck, (n.d.). <https://www.sigmaaldrich.com/FR/en> (accessed September 28, 2021).
- [40] ChemSpider, (n.d.). <http://www.chemspider.com/> (accessed September 28, 2021).
- [41] V. Knop, M. Loos, C. Pera, N. Jeuland, A linear-by-mole blending rule for octane numbers of n-heptane/iso-octane/toluene mixtures, *Fuel.* 115 (2014) 666–673. <https://doi.org/10.1016/j.fuel.2013.07.093>.
- [42] PubChem, PubChem, (n.d.). <https://pubchem.ncbi.nlm.nih.gov/> (accessed January 31, 2022).
- [43] S.K. Garg, T.S. Banipal, J.C. Ahluwalia, Heat capacities and densities of liquid o-xylene, m-xylene, p-xylene, and ethylbenzene, at temperatures from 318.15 K to 373.15 K and at pressures up to 10 MPa, *The Journal of Chemical Thermodynamics.* 25 (1993) 57–62. <https://doi.org/10.1006/jcht.1993.1007>.
- [44] European committee for standardization, European Standard EN 228 - Automotive fuels - Unleaded petrol - Requirements and test methods, (2008). http://www.envirochem.hu/www.envirochem.hu/documents/EN_228_benzin_JBg37.pdf.
- [45] Comité Professionnel Du Pétrole, EN 590, (2005). https://www.matevi-france.com/fileadmin/user_upload/fichiers_matevi/_PDF/informations_pratiques/Norme-EN-590-2004.pdf.
- [46] NIST WebBook, (n.d.). <https://webbook.nist.gov/chemistry/> (accessed September 28, 2021).
- [47] M.A. Ratcliff, J. Burton, P. Sindler, E. Christensen, L. Fouts, G.M. Chupka, R.L. McCormick, Knock Resistance and Fine Particle Emissions for Several Biomass-Derived Oxygenates in a Direct-Injection Spark-Ignition Engine, *SAE International Journal of Fuels and Lubricants.* 9 (2016) 59–70.
- [48] M. Tian, Lignocellulosic octane boosters, Technische Universiteit Eindhoven, 2016. https://pure.tue.nl/ws/portalfiles/portal/41981681/20161107_Tian.pdf.
- [49] J.P. Szybist, D.A. Splitter, Understanding chemistry-specific fuel differences at a constant RON in a boosted SI engine, *Fuel.* 217 (2018) 370–381. <https://doi.org/10.1016/j.fuel.2017.12.100>.
- [50] R.L. McCormick, G. Fioroni, L. Fouts, E. Christensen, J. Yanowitz, E. Polikarpov, K. Albrecht, D.J. Gaspar, J. Gladden, A. George, Selection Criteria and Screening of

- Potential Biomass-Derived Streams as Fuel Blendstocks for Advanced Spark-Ignition Engines, *SAE International Journal of Fuels and Lubricants*. 10 (2017) 442–460. <https://doi.org/10.4271/2017-01-0868>.
- [51] K.G. Joback, R.C. Reid, Estimation of pure-component properties from group-contributions, *Chemical Engineering Communications*. (2007). <https://doi.org/10.1080/00986448708960487>.
- [52] GuideChem, (n.d.). <https://www.guidechem.com/trade/2-3-benzofuran-id5300001.html> (accessed February 28, 2022).
- [53] T.E. Daubert, *Physical and thermodynamic properties of pure chemicals: data compilation*, Taylor & Francis, Washington, DC, 1989.
- [54] V.S.B. Shankar, M. Al-Abbad, M. El-Rachidi, S.Y. Mohamed, E. Singh, Z. Wang, A. Farooq, S.M. Sarathy, Antiknock quality and ignition kinetics of 2-phenylethanol, a novel lignocellulosic octane booster, *Proceedings of the Combustion Institute*. 36 (2017) 3515–3522. <https://doi.org/10.1016/j.proci.2016.05.041>.
- [55] Y. Li, K. Nithyanandan, X. Meng, T.H. Lee, Y. Li, C.F. Lee, Z. Ning, Experimental study on combustion and emission performance of a spark-ignition engine fueled with water containing acetone-gasoline blends, *Fuel*. 210 (2017) 133–144. <https://doi.org/10.1016/j.fuel.2017.07.058>.
- [56] SpectraBase, (n.d.). <https://spectrabase.com/spectrum/6HOPJ2iWOU> (accessed March 29, 2022).
- [57] R.D. Büttgen, M. Tian, Y. Fenard, H. Minwegen, M.D. Boot, K.A. Heufer, An experimental, theoretical and kinetic modelling study on the reactivity of a lignin model compound anisole under engine-relevant conditions, *Fuel*. 269 (2020) 117190. <https://doi.org/10.1016/j.fuel.2020.117190>.
- [58] Parchem, (n.d.). <https://www.parchem.com/chemical-supplier-distributor/3-ETHYLPHENOL-033256.aspx> (accessed February 28, 2022).
- [59] Echemi, (n.d.). https://www.echemi.com/products/pid_Seven1656-4-n-propylanisole.html (accessed January 31, 2022).
- [60] I. Fonts, M. Atienza-Martínez, H.-H. Carstensen, M. Benés, A.P. Pinheiro Pires, M. Garcia-Perez, R. Bilbao, Thermodynamic and Physical Property Estimation of Compounds Derived from the Fast Pyrolysis of Lignocellulosic Materials, *Energy Fuels*. 35 (2021) 17114–17137. <https://doi.org/10.1021/acs.energyfuels.1c01709>.
- [61] S. Hosseinpour, M. Aghbashlo, M. Tabatabaei, E. Khalife, Exact estimation of biodiesel cetane number (CN) from its fatty acid methyl esters (FAMES) profile using partial least square (PLS) adapted by artificial neural network (ANN), *Energy Conversion and Management*. 124 (2016) 389–398. <https://doi.org/10.1016/j.enconman.2016.07.027>.
- [62] A.M. Schweidtmann, J.G. Rittig, A. König, M. Grohe, A. Mitsos, M. Dahmen, Graph Neural Networks for Prediction of Fuel Ignition Quality, *Energy Fuels*. 34 (2020) 11395–11407. <https://doi.org/10.1021/acs.energyfuels.0c01533>.

- [63] A.G. Abdul Jameel, V. Van Oudenhoven, A.-H. Emwas, S.M. Sarathy, Predicting Octane Number Using Nuclear Magnetic Resonance Spectroscopy and Artificial Neural Networks, *Energy Fuels*. 32 (2018) 6309–6329. <https://doi.org/10.1021/acs.energyfuels.8b00556>.
- [64] H.G. Aleme, P.J.S. Barbeira, Determination of flash point and cetane index in diesel using distillation curves and multivariate calibration, *Fuel*. 102 (2012) 129–134. <https://doi.org/10.1016/j.fuel.2012.06.015>.
- [65] J.B. Cooper, K.L. Wise, James. Groves, W.T. Welch, Determination of Octane Numbers and Reid Vapor Pressure of Commercial Petroleum Fuels Using FT-Raman Spectroscopy and Partial Least-Squares Regression Analysis, *Anal. Chem.* 67 (1995) 4096–4100. <https://doi.org/10.1021/ac00118a011>.
- [66] A. Bemani, Q. Xiong, A. Baghban, S. Habibzadeh, A.H. Mohammadi, M.H. Doranehgard, Modeling of cetane number of biodiesel from fatty acid methyl ester (FAME) information using GA-, PSO-, and HGAPSO- LSSVM models, *Renewable Energy*. 150 (2020) 924–934. <https://doi.org/10.1016/j.renene.2019.12.086>.
- [67] A. Baghban, M. Adelizadeh, On the determination of cetane number of hydrocarbons and oxygenates using Adaptive Neuro Fuzzy Inference System optimized with evolutionary algorithms, *Fuel*. 230 (2018) 344–354. <https://doi.org/10.1016/j.fuel.2018.05.032>.
- [68] N. Naser, S.M. Sarathy, S.H. Chung, Estimating fuel octane numbers from homogeneous gas-phase ignition delay times - ScienceDirect, *Combust. Flame*. 188 (2018) 307–323. <https://doi.org/10.1016/j.combustflame.2017.09.037>.
- [69] V. Mathan Raj, L.R. Ganapathy Subramanian, S. Thiyagarajan, V. Edwin Geo, Effects of minor addition of aliphatic (1-pentanol) and aromatic (benzyl alcohol) alcohols in Simarouba Glauca-diesel blend fuelled CI engine, *Fuel*. 234 (2018) 934–943. <https://doi.org/10.1016/j.fuel.2018.07.122>.
- [70] K. Hashimoto, T. Kudo, T. Sato, I. Takase, T. Suzuki, T. Nakano, On Demand Octane Number Enhancement Technology by Aerobic Oxidation, SAE International, Warrendale, PA, 2016. <https://doi.org/10.4271/2016-01-2167>.
- [71] K. Cho, C.-H. Lee, K. Ko, Y.-J. Lee, K.-N. Kim, M.-K. Kim, Y.-H. Chung, D. Kim, I.-K. Yeo, T. Oda, Use of phenol-induced oxidative stress acclimation to stimulate cell growth and biodiesel production by the oceanic microalga *Dunaliella salina*, *Algal Research*. 17 (2016) 61–66. <https://doi.org/10.1016/j.algal.2016.04.023>.
- [72] J.D. Cox, The heats of combustion of phenol and the three cresols, *Pure and Applied Chemistry*. 2 (1961) 125–128. <https://doi.org/10.1351/pac196102010125>.
- [73] L. Zhou, M.D. Boot, B.H. Johansson, J.J.E. Reijnders, Performance of lignin derived aromatic oxygenates in a heavy-duty diesel engine, *Fuel*. 115 (2014) 469–478. <https://doi.org/10.1016/j.fuel.2013.07.047>.

- [74] L. Zhou, M.D. Boot, L.P.H. de Goey, Gasoline - Ignition Improver - Oxygenate Blends as Fuels for Advanced Compression Ignition Combustion, SAE International, Warrendale, PA, 2013. <https://doi.org/10.4271/2013-01-0529>.
- [75] Y. Wu, B. Rossow, V. Modica, X. Yu, L. Wu, F. Grisch, Laminar flame speed of lignocellulosic biomass-derived oxygenates and blends of gasoline/oxygenates, *Fuel*. 202 (2017) 572–582. <https://doi.org/10.1016/j.fuel.2017.04.085>.
- [76] A.G. Abdul Jameel, A functional group approach for predicting fuel properties, King Abdullah University of Science and Technology, 2019. <https://repository.kaust.edu.sa/handle/10754/631722> (accessed September 28, 2021).
- [77] G. da Silva, J.W. Bozzelli, On the reactivity of methylbenzenes, *Combustion and Flame*. 157 (2010) 2175–2183. <https://doi.org/10.1016/j.combustflame.2010.06.001>.
- [78] J. Yanowitz, M.A. Ratcliff, R.L. McCormick, J.D. Taylor, M.J. Murphy, Compendium of Experimental Cetane Numbers, National Renewable Energy Lab. (NREL), Golden, CO (United States), 2017. <https://doi.org/10.2172/1345058>.
- [79] EnggCyclopedia, (2011). <https://www.enggcyclopedia.com/2011/09/heating-values-natural-gas/> (accessed September 28, 2021).
- [80] D.S.J. Jones, P.P. Pujadó, Handbook of Petroleum Processing, Springer Science & Business Media, 2006.
- [81] N. Morgan, A. Smallbone, A. Bhave, M. Kraft, R. Cracknell, G. Kalghatgi, Mapping surrogate gasoline compositions into RON/MON space, *Combustion and Flame*. 157 (2010) 1122–1131. <https://doi.org/10.1016/j.combustflame.2010.02.003>.
- [82] T.M. Foong, K.J. Morganti, M.J. Brear, G. da Silva, Y. Yang, F.L. Dryer, The octane numbers of ethanol blended with gasoline and its surrogates, *Fuel*. 115 (2014) 727–739. <https://doi.org/10.1016/j.fuel.2013.07.105>.
- [83] J. Coops, D.M. Jmzn, J.W. Dieneske, J. Smittenberg, The heats of combustion of a number of hydrocarbons, *Recueil Des Travaux Chimiques Des Pays-Bas*. 65 (1946) 128–128. <https://doi.org/10.1002/recl.19460650213>.
- [84] E.J. Prosen, R. Gilmont, F.D. Rossini, Heats of combustion of benzene, toluene, ethylbenzene, o-xylene, m-xylene, p-xylene, n-propylbenzene, and styrene, *J. RES. NATL. BUR. STAN*. 34 (1945) 65. <https://doi.org/10.6028/jres.034.034>.
- [85] L.S. Tran, B. Sirjean, P.-A. Glaude, R. Fournet, F. Battin-Leclerc, Progress in detailed kinetic modeling of the combustion of oxygenated components of biofuels, *Energy*. 43 (2012) 4–18. <https://doi.org/10.1016/j.energy.2011.11.013>.
- [86] CHEMKIN 10112, Reaction Design, San Diego, 2011.
- [87] D. Goodwin, R. Speth, H. Moffat, B. Weber, Cantera: An object-oriented software toolkit for chemical kinetics, thermodynamics, and transport processes, (2021). <https://doi.org/10.5281/zenodo.4527812>.

- [88] A. Stagni, A. Cuoci, A. Frassoldati, T. Faravelli, E. Ranzi, Lumping and Reduction of Detailed Kinetic Schemes: an Effective Coupling, *Ind. Eng. Chem. Res.* 53 (2014) 9004–9016. <https://doi.org/10.1021/ie403272f>.
- [89] J. Herzler, M. Fikri, C. Schulz, Ignition Delay Time Study of Aromatic LIF Tracers in a Wide Temperature and Pressure Range, 26th ICDERS, Boston, MA. (2017) 6.
- [90] R. Fang, C.-J. Sung, A Rapid Compression Machine Study of 2-Phenylethanol Autoignition at Low-To-Intermediate Temperatures, *Energies*. 14 (2021) 7708. <https://doi.org/10.3390/en14227708>.
- [91] S.W. Wagnon, S. Thion, E.J.K. Nilsson, M. Mehl, Z. Serinyel, K. Zhang, P. Dagaut, A.A. Konnov, G. Dayma, W.J. Pitz, Experimental and modeling studies of a biofuel surrogate compound: laminar burning velocities and jet-stirred reactor measurements of anisole, *Combust. Flame*. 189 (2018) 325–336. <https://doi.org/10.1016/j.combustflame.2017.10.020>.
- [92] S. Zare, S. Roy, A. El Maadi, O. Askari, An investigation on laminar burning speed and flame structure of anisole-air mixture, *Fuel*. 244 (2019) 120–131. <https://doi.org/10.1016/j.fuel.2019.01.149>.
- [93] A.G. Gaydon, I.R. Hurle, The shock tube in high-temperature chemical physics, *J. Chem. Educ.* 41 (1964) 114. <https://doi.org/10.1021/ed041p114.3>.
- [94] S.S. Goldsborough, S. Hochgreb, G. Vanhove, M.S. Wooldridge, H.J. Curran, C.-J. Sung, Advances in rapid compression machine studies of low- and intermediate-temperature autoignition phenomena, *Prog. Energ. Combust.* 63 (2017) 1–78. <https://doi.org/10.1016/j.pecs.2017.05.002>.
- [95] B.M. Gauthier, D.F. Davidson, R.K. Hanson, Shock tube determination of ignition delay times in full-blend and surrogate fuel mixtures, *Combustion and Flame*. 139 (2004) 300–311. <https://doi.org/10.1016/j.combustflame.2004.08.015>.
- [96] C.S. Mergulhão, H.-H. Carstensen, H. Song, S.W. Wagnon, W.J. Pitz, G. Vanhove, Probing the antiknock effect of anisole through an ignition, speciation and modeling study of its blends with isooctane, *Proceedings of the Combustion Institute*. 38 (2021) 739–748. <https://doi.org/10.1016/j.proci.2020.08.013>.
- [97] A.A. Konnov, A. Mohammad, V.R. Kishore, N.I. Kim, C. Prathap, S. Kumar, A comprehensive review of measurements and data analysis of laminar burning velocities for various fuel+air mixtures, *Progress in Energy and Combustion Science*. 68 (2018) 197–267. <https://doi.org/10.1016/j.pecs.2018.05.003>.
- [98] Goey, de L.P.H., Maaren, van A., Quax, R.M., Mechanical Engineering, Group De Goey, Stabilization of adiabatic premixed laminar flames on a flat flame burner, *Combustion Science and Technology*. 92 (1993) 201–207. <https://doi.org/10.1080/00102209308907668>.
- [99] D.D. Das, P.C. St. John, C.S. McEnally, S. Kim, L.D. Pfefferle, Measuring and predicting sooting tendencies of oxygenates, alkanes, alkenes, cycloalkanes, and aromatics on a

- unified scale, *Combustion and Flame*. 190 (2018) 349–364. <https://doi.org/10.1016/j.combustflame.2017.12.005>.
- [100] Y. Kim, B.D. Etz, G.M. Fioroni, C.K. Hays, P.C. St. John, R.A. Messerly, S. Vyas, B.P. Beekley, F. Guo, C.S. McEnally, L.D. Pfefferle, R.L. McCormick, S. Kim, Investigation of structural effects of aromatic compounds on sooting tendency with mechanistic insight into ethylphenol isomers, *Proceedings of the Combustion Institute*. 38 (2021) 1143–1151. <https://doi.org/10.1016/j.proci.2020.06.321>.
- [101] R.H. Schlosberg, P.F. Szajowski, G.D. Dupre, J.A. Danik, A. Kurs, T.R. Ashe, W.I. Olmstead, Pyrolysis studies of organic oxygenates: 3. High temperature rearrangement of aryl alkyl ethers, *Fuel (Guildford)*. 62 (1983) 690–694. [https://doi.org/10.1016/0016-2361\(83\)90308-3](https://doi.org/10.1016/0016-2361(83)90308-3).
- [102] R. Ceylan, J. Bredenberg, Hydrogenolysis and hydrocracking of the carbon-oxygen bond. 2. Thermal cleavage of the carbon-oxygen bond in guaiacol, *Fuel (Guildford)*. 61 (1982) 377–382. [https://doi.org/10.1016/0016-2361\(82\)90054-0](https://doi.org/10.1016/0016-2361(82)90054-0).
- [103] M.T. Klein, Model pathways in lignin thermolysis, Massachusetts Institute of Technology, 1981.
- [104] J.R. Lawson, M.T. Klein, Influence of water on guaiacol pyrolysis, *Ind. Eng. Chem. Fund.* 24 (1985) 203–208. <https://doi.org/10.1021/i100018a012>.
- [105] R. Taylor, The Mechanism of Thermal Eliminations. Part 25. Arrhenius Data for Pyrolysis of Isochroman-3-one, Benzyl Methyl Ether, 2-Hydroxyethylbenzene, Phenyl Acetate, and 3,4-Dihydro-ZH-pyran, *J. CHEM. SOC. PERKIN TRANS.* 2 (1988) 183–189. <https://doi.org/10.1039/p29880000183>.
- [106] G. Chuchani, A. Rotinov, R.M. Dominguez, The kinetics and mechanisms of gas phase elimination of primary, secondary, and tertiary 2-hydroxyalkylbenzenes, *International Journal of Chemical Kinetics*. 31 (1999) 401–407. [https://doi.org/10.1002/\(SICI\)1097-4601\(1999\)31:6<401::AID-KIN1>3.0.CO;2-Z](https://doi.org/10.1002/(SICI)1097-4601(1999)31:6<401::AID-KIN1>3.0.CO;2-Z).
- [107] A.B. Lovell, K. Brezinsky, I. Glassman, The gas phase pyrolysis of phenol, *International Journal of Chemical Kinetics*. 21 (1989) 547–560. <https://doi.org/10.1002/kin.550210706>.
- [108] J.A. Manion, R. Louw, Rates, products, and mechanisms in the gas-phase hydrogenolysis of phenol between 922 and 1175 K, *J. Phys. Chem.* 93 (1989) 3563–3574. <https://doi.org/10.1021/j100346a040>.
- [109] C. Horn, K. Roy, P. Frank, T. Just, Shock-tube study on the high-temperature pyrolysis of phenol, *Symposium (International) on Combustion*. 27 (1998) 321–328. [https://doi.org/10.1016/S0082-0784\(98\)80419-0](https://doi.org/10.1016/S0082-0784(98)80419-0).
- [110] K. Brezinsky, M. Pecullan, I. Glassman, Pyrolysis and Oxidation of Phenol, *J. Phys. Chem. A*. 102 (1998) 8614–8619. <https://doi.org/10.1021/jp982177+>.
- [111] E.B. Ledesma, N.D. Marsh, A.K. Sandrowitz, M.J. Wornat, An experimental study on the thermal decomposition of catechol, *Proceedings of the Combustion Institute*. 29 (2002) 2299–2306. [https://doi.org/10.1016/S1540-7489\(02\)80280-2](https://doi.org/10.1016/S1540-7489(02)80280-2).

- [112] S. Thomas, E.B. Ledesma, M.J. Wornat, The effects of oxygen on the yields of the thermal decomposition products of catechol under pyrolysis and fuel-rich oxidation conditions, *Fuel*. 86 (2007) 2581–2595. <https://doi.org/10.1016/j.fuel.2007.02.003>.
- [113] S. Namysl, M. Pelucchi, L. Pratali Maffei, O. Herbinet, A. Stagni, T. Faravelli, F. Battin-Leclerc, Experimental and modeling study of benzaldehyde oxidation, *Combust. Flame*. 211 (2020) 124–132. <https://doi.org/10.1016/j.combustflame.2019.09.024>.
- [114] J.-T. Chen, D. Yu, W. Li, W.-Y. Chen, S.-B. Song, C. Xie, J.-Z. Yang, Z.-Y. Tian, Oxidation study of benzaldehyde with synchrotron photoionization and molecular beam mass spectrometry, *Combustion and Flame*. 220 (2020) 455–467. <https://doi.org/10.1016/j.combustflame.2020.07.019>.
- [115] C.-Y. Lin, M.C. Lin, Thermal decomposition of methyl phenyl ether in shock waves: the kinetics of phenoxy radical reactions, *J. Phys. Chem.* 90 (1986) 425–431. <https://doi.org/10.1021/j100275a014>.
- [116] S. Zabeti, M. Aghsaee, M. Fikri, O. Welz, C. Schulz, Optical properties and pyrolysis of shock-heated gas-phase anisole, *Proceedings of the Combustion Institute*. 36 (2017) 4525–4532. <https://doi.org/10.1016/j.proci.2016.06.156>.
- [117] I.W.C.E. Arends, R. Louw, P. Mulder, Kinetic study of the thermolysis of anisole in a hydrogen atmosphere, *J. Phys. Chem.* 97 (1993) 7914–7925. <https://doi.org/10.1021/j100132a020>.
- [118] M. Pecullan, K. Brezinsky, I. Glassman, Pyrolysis and Oxidation of Anisole near 1000 K, *J. Phys. Chem. A*. 101 (1997) 3305–3316. <https://doi.org/10.1021/jp963203b>.
- [119] V.V. Platonov, V.A. Proskuryakov, S.V. Ryl'tsova, Yu.N. Popova, Homogeneous Pyrolysis of Anisole, *Russian Journal of Applied Chemistry*. 74 (2001) 1047–1052. <https://doi.org/10.1023/A:1013076330586>.
- [120] A.V. Friderichsen, E.-J. Shin, R.J. Evans, M.R. Nimlos, D.C. Dayton, G.B. Ellison, The pyrolysis of anisole (C₆H₅OCH₃) using a hyperthermal nozzle, *Fuel*. 80 (2001) 1747–1755. [https://doi.org/10.1016/S0016-2361\(01\)00059-X](https://doi.org/10.1016/S0016-2361(01)00059-X).
- [121] Pelucchi M., Faravelli T., Frassoldati A., Ranzi E., SriBala G., Marin G., Van Geem K., Experimental and kinetic modeling study of pyrolysis and combustion of anisole., *Chemical Engineering Transactions*. 65 (2018) 127–132. <https://doi.org/10.3303/CET1865022>.
- [122] W. Yuan, T. Li, Y. Li, M. Zeng, Y. Zhang, J. Zou, C. Cao, W. Li, J. Yang, F. Qi, Experimental and kinetic modeling investigation on anisole pyrolysis: Implications on phenoxy and cyclopentadienyl chemistry, *Combustion and Flame*. 201 (2019) 187–199. <https://doi.org/10.1016/j.combustflame.2018.12.028>.
- [123] J.C. Mackie, M.B. Colket, P.F. Nelson, Shock tube pyrolysis of pyridine, *J. Phys. Chem.* 94 (1990) 4099–4106. <https://doi.org/10.1021/j100373a040>.
- [124] M. Nowakowska, O. Herbinet, A. Dufour, P.-A. Glaude, Detailed kinetic study of anisole pyrolysis and oxidation to understand tar formation during biomass combustion

- and gasification, *Combustion and Flame*. 161 (2014) 1474–1488. <https://doi.org/10.1016/j.combustflame.2013.11.024>.
- [125] T. Bierkandt, P. Hemberger, P. Oßwald, D. Krüger, M. Köhler, T. Kasper, Flame structure of laminar premixed anisole flames investigated by photoionization mass spectrometry and photoelectron spectroscopy, *Proceedings of the Combustion Institute*. 37 (2019) 1579–1587. <https://doi.org/10.1016/j.proci.2018.07.037>.
- [126] B. Chen, M. Hellmuth, S. Faller, L. May, P. Liu, L. Cai, W.L. Roberts, H. Pitsch, Exploring the combustion chemistry of anisole in laminar counterflow diffusion-flames under oxy-fuel conditions, *Combustion and Flame*. (2021) 111929. <https://doi.org/10.1016/j.combustflame.2021.111929>.
- [127] L. Zhou, D. Yu, Z. Wang, L.-J. Cheng, Z.-H. Jin, J.-J. Weng, J.-Z. Yang, Z.-Y. Tian, A detailed kinetic study on oxidation of benzyl alcohol, *Combustion and Flame*. 207 (2019) 10–19. <https://doi.org/10.1016/j.combustflame.2019.05.034>.
- [128] J.-T. Chen, Z.-H. Jin, W. Li, K.-R. Jin, S.-B. Song, J.-Z. Yang, Z.-Y. Tian, Experimental and kinetic modeling study of benzyl alcohol pyrolysis, *Combustion and Flame*. 231 (2021) 111477. <https://doi.org/10.1016/j.combustflame.2021.111477>.
- [129] M. Nowakowska, O. Herbinet, A. Dufour, P.A. Glaude, Kinetic Study of the Pyrolysis and Oxidation of Guaiacol, *J. Phys. Chem. A*. 122 (2018) 7894–7909. <https://doi.org/10.1021/acs.jpca.8b06301>.
- [130] A. Yerrayya, U. Natarajan, R. Vinu, Fast pyrolysis of guaiacol to simple phenols: Experiments, theory and kinetic model, *Chemical Engineering Science*. 207 (2019) 619–630. <https://doi.org/10.1016/j.ces.2019.06.025>.
- [131] B.D. Etz, G.M. Fioroni, R.A. Messerly, M.J. Rahimi, P.C. St. John, D.J. Robichaud, E.D. Christensen, B.P. Beekley, C.S. McEnally, L.D. Pfefferle, Y. Xuan, S. Vyas, R.S. Paton, R.L. McCormick, S. Kim, Elucidating the chemical pathways responsible for the sooting tendency of 1 and 2-phenylethanol, *Proceedings of the Combustion Institute*. 38 (2021) 1327–1334. <https://doi.org/10.1016/j.proci.2020.06.072>.
- [132] F. Monge, V. Aranda, A. Millera, R. Bilbao, M.U. Alzueta, Tubular Flow Reactors, in: F. Battin-Leclerc, J.M. Simmie, E. Blurock (Eds.), *Cleaner Combustion: Developing Detailed Chemical Kinetic Models*, Springer, London, 2013: pp. 211–230. https://doi.org/10.1007/978-1-4471-5307-8_9.
- [133] O. Herbinet, D. Guillaume, Jet-Stirred Reactors, in: F. Battin-Leclerc, J.M. Simmie, E. Blurock (Eds.), *Cleaner Combustion: Developing Detailed Chemical Kinetic Models*, Springer, 2013: pp. 183–210. <https://doi.org/10.1007/978-1-4471-5307-8>.
- [134] F.N. Egolfopoulos, N. Hansen, Y. Ju, K. Kohse-Höinghaus, C.K. Law, F. Qi, Advances and challenges in laminar flame experiments and implications for combustion chemistry, *Progress in Energy and Combustion Science*. 43 (2014) 36–67. <https://doi.org/10.1016/j.pecs.2014.04.004>.

- [135] Y.Z. He, W.G. Mallard, W. Tsang, Kinetics of hydrogen and hydroxyl radical attack on phenol at high temperatures, *J. Phys. Chem.* 92 (1988) 2196–2201. <https://doi.org/10.1021/j100319a023>.
- [136] R. Bounaceur, I. Da Costa, R. Fournet, F. Billaud, F. Battin-Leclerc, Experimental and modeling study of the oxidation of toluene, *International Journal of Chemical Kinetics*. 37 (2005) 25–49. <https://doi.org/10.1002/kin.20047>.
- [137] R.I. Kaiser, L. Zhao, W. Lu, M. Ahmed, M.V. Zagidullin, V.N. Azyazov, A.M. Mebel, Formation of Benzene and Naphthalene through Cyclopentadienyl-Mediated Radical–Radical Reactions, *J. Phys. Chem. Lett.* 13 (2022) 208–213. <https://doi.org/10.1021/acs.jpcclett.1c03733>.
- [138] J.W. Martin, Soot inception: Carbonaceous nanoparticle formation in flames, *Progress in Energy and Combustion Science*. 88 (2022) 100956. <https://doi.org/10.1016/j.pecs.2021.100956>.
- [139] M.J. Wornat, E.B. Ledesma, N.D. Marsh, Polycyclic aromatic hydrocarbons from the pyrolysis of catechol (ortho-dihydroxybenzene), a model fuel representative of entities in tobacco, coal, and lignin, *Fuel*. 80 (2001) 1711–1726. [https://doi.org/10.1016/S0016-2361\(01\)00057-6](https://doi.org/10.1016/S0016-2361(01)00057-6).
- [140] C.D. Hurd, C.W. Bennett, The pyrolysis of benzaldehyde and of benzyl benzoate, *J. Am. Chem. Soc.* 51 (1929) 1197–1201. <https://doi.org/10.1021/ja01379a030>.
- [141] M.A. Grela, A.J. Colussi, Kinetics and mechanism of the thermal decomposition of unsaturated aldehydes: benzaldehyde, 2-butenal, and 2-furaldehyde, *J. Phys. Chem.* 90 (1986) 434–437. <https://doi.org/10.1021/j100275a016>.
- [142] S.L. Bruinsma, R.S. Geertsma, P. Bank, A. Moulijn, Gas phase pyrolysis of coal-related aromatic compounds in a coiled tube flow reactor, *FUEL*. 67 (1988) 327–333.
- [143] A.K. Vasiliou, J.H. Kim, T.K. Ormond, K.M. Piech, K.N. Urness, A.M. Scheer, D.J. Robichaud, C. Mukarakate, M.R. Nimlos, J.W. Daily, Q. Guan, H.-H. Carstensen, G.B. Ellison, Biomass pyrolysis: Thermal decomposition mechanisms of furfural and benzaldehyde, *The Journal of Chemical Physics*. 139 (2013) 104310. <https://doi.org/10.1063/1.4819788>.
- [144] M.F.R. Mulcahy, B.G. Tucker, D.J. Williams, J.R. Wilmshurst, Reactions of free radicals with aromatic compounds in the gaseous phase. III. Kinetics of the reaction of methyl radicals with anisole (methoxybenzene), *Aust. J. Chem.* 20 (1967) 1155–1171. <https://doi.org/10.1071/ch9671155>.
- [145] S.W. Wagnon, S. Thion, E.J.K. Nilsson, M. Mehl, Z. Serinyel, K. Zhang, P. Dagaut, A.A. Konnov, G. Dayma, W.J. Pitz, Experimental and modeling studies of a biofuel surrogate compound: laminar burning velocities and jet-stirred reactor measurements of anisole, *Combustion and Flame*. 189 (2018) 325–336. <https://doi.org/10.1016/j.combustflame.2017.10.020>.

- [146] A.M. Scheer, C. Mukarakate, D.J. Robichaud, M.R. Nimlos, G.B. Ellison, Thermal Decomposition Mechanisms of the Methoxyphenols: Formation of Phenol, Cyclopentadienone, Vinylacetylene, and Acetylene, *J. Phys. Chem. A*. 115 (2011) 13381–13389. <https://doi.org/10.1021/jp2068073>.
- [147] M.K. Singh, K.P.J. Reddy, E. Arunan, Shock Tube Experimental and Theoretical Study on the Thermal Decomposition of 2-Phenylethanol, in: G. Ben-Dor, O. Sadot, O. Igra (Eds.), 30th International Symposium on Shock Waves 1, Springer International Publishing, Cham, 2017: pp. 317–320. https://doi.org/10.1007/978-3-319-46213-4_53.
- [148] E. Ghibaudi, A.J. Colussi, Very low pressure pyrolysis of phenyl acetate, *International Journal of Chemical Kinetics*. 16 (1984) 1575–1583.
- [149] L. Pratali Maffei, M. Pelucchi, T. Faravelli, C. Cavallotti, Theoretical study of sensitive reactions in phenol decomposition, *React. Chem. Eng.* 5 (2020) 452–472. <https://doi.org/10.1039/C9RE00418A>.
- [150] Y. Zhang, K.P. Somers, M. Mehl, W.J. Pitz, R.F. Cracknell, H.J. Curran, Probing the antagonistic effect of toluene as a component in surrogate fuel models at low temperatures and high pressures. A case study of toluene/dimethyl ether mixtures, *Proceedings of the Combustion Institute*. 36 (2017) 413–421. <https://doi.org/10.1016/j.proci.2016.06.190>.
- [151] H. Ning, J. Wu, L. Ma, W. Ren, Exploring the pyrolysis chemistry of prototype aromatic ester phenyl formate: Reaction pathways, thermodynamics and kinetics, *Combustion and Flame*. 211 (2020) 337–346. <https://doi.org/10.1016/j.combustflame.2019.10.002>.
- [152] E. Ranzi, A. Cuoci, T. Faravelli, A. Frassoldati, G. Migliavacca, S. Pierucci, S. Sommariva, Chemical Kinetics of Biomass Pyrolysis, *Energy Fuels*. 22 (2008) 4292–4300. <https://doi.org/10.1021/ef800551t>.
- [153] M. Pelucchi, C. Cavallotti, A. Cuoci, T. Faravelli, A. Frassoldati, E. Ranzi, Detailed kinetics of substituted phenolic species in pyrolysis bio-oils, *React. Chem. Eng.* 4 (2019) 490–506. <https://doi.org/10.1039/C8RE00198G>.